Optimal Design and Operation of an Industrial Fluidized Catalytic Cracking Reactor

Aysar T. Jarullah[1,2] , Noor A. Awad[1], Iqbal M. Mujtaba[3]

[1] Chemical Engineering Department, College of Engineering, Tikrit University

[2] Email: A.T.Jarullah@tu.edu.iq

[3] Chemical Engineering Division, School of Engineering, University of Bradford, Bradford BD7 1DP UK

[3] Email: I.M.Mujtaba@bradford.ac.uk

Abstract

Fluidized catalytic cracking (FCC) is regarded one of the most significant operations in the oil refining industries to convert feedstock (mainly vacuum gasoil) to valuable products (namely gasoline and diesel). The behavior of the fluidized catalytic cracking process is playing a main part on the overall benefits of refinery units and improving in process or control of fluidized catalytic cracking plants will result in exciting benefits economically. According to these highlights, this study is aimed to develop a new mathematical model for the FCC process taking into account the complex hydrodynamics of the reactor regenerator system with a new six lumps kinetic model for the riser. The mathematical model, simulation and optimization have done utilizing vacuum gas oil (VGO) as a feedstock and zeolite as a catalyst under the following operating conditions: temperature (733K, 783K, and 813K), weight hourly space velocity (5, 20 and 30hr^{-1}) and catalyst to oil ratio (4, 7 and 10). The best kinetic parameters of the relevant reactions are estimated using the optimization technique based on the experimental results taken from literature. The effect of operating condition (mainly, reaction temp (T), catalyst to oil ratio (CTO) and weight hourly space velocity (WHSV) on the product composition has also been discussed. The optimal kinetic parameters obtained from the pilot plant scale have been employed to develop an industrial FCC process, where optimal operating condition based on maximum conversion of VGO with minimum cost in addition to maximizing the octane number of gasoline (GLN), have been studied. Minimum coke content deposition the catalyst within the regenerator is also investigated here. New results (the highest conversion and octane number, and the lowest coke content) have obtained in comparison with those reported in the literature.

1. Introduction

Cracking is the process where the large undesirable compounds break down into smaller compounds and extra beneficial molecules. Such process is conducted without catalyst at high reaction temperature (T) and pressure (P), or with the catalyst at low or moderate T and P. Based on the market request, oil industries have used the FCC processes for the purpose of increasing the valuable products (mainly car fuels) and decreasing the heavy oil fractions obtained by oil distillation. The riser reactors of the fluidized catalytic cracking process have designed based on acidic catalyst, where heavy cuts (namely reduced crude residue and vacuum gas oil (VGO)) are decomposed into more valuable products at a specified process conditions. Also, the quality of the products in the reactors depends on the operating conditions and such products can be improved via changing the process conditions **(Werther and Hirschberg, 1997;**

Jin et al., 2002). Recently, the worldwide is producing approximate 45% of the car fuel (gasoline) via fluidized catalytic cracking plants (directly) in addition to other supplementary process (indirectly) such as alkylation process **(Chen, 2006).** During 2006, fluidized catalytic cracking process have reported at 400 oil industries and about 1/3 of those petroleum refining companies were operated in the fluidized catalytic cracking process resulting car fuel with higher-octane number (ON) and engine fuels **(Jones and Pujadó, 2006)**. In 2007, the fluidized catalytic cracking plants in the USA has been processed a total of 8343×10^8 m^3/day of feedstock, while double amount of such feedstock has been processed other countries **(Pradhan, 2012).**

The fluidized catalytic cracking operating have improved as a results of evolving in petroleum refining industries in the last decades, achieving the goals expected of improving heavier, to more contaminate feed stocks, to increase process flexibility accommodating environmental regulation in addition to maximize reliability **(Meyers, 2004)**. According to the environmental impact, fluidized catalytic cracking process has played an important factor via production car fuel with lower benzene content **(Colorado school of mines, 2016).** The thermal cracking (THC) process (using T and P without catalyst) and catalytic cracking (CAC) process (similar to THC with catalyst to produce light compound from heavy compounds) are considered the main cracking processes. Using catalysts in CAC reaction can increase the yield and improves the products quality a moderate or lower process conditions in comparison to THE process, which mean that the car fuels with higher ON, lower heavy fuel oils in addition to light gases (LG) are obtained. The LG obtained by CAC process contains higher olefin compounds than those obtained by THE process **(James et al., 2001).**

In this study, a mathematical process model is developed which can accurately simulate industrial FCC reactor. The reaction kinetic models are developed based on six lump models and experimental data taking hydrodynamic factors into consideration. The model is then employed to optimize the process conditions of the operation which will maximize the conversion and the octane number while minimizing the cock content in the regenerator.

2. FCC Process

At the conventional process, the VGO and any feedstock is heated utilizing the heat generated via main fractionators bottoms pump around and/or fired heaters. The feedstock of fluidized catalytic cracking process is heated earlier and then channeled to the reactor to meet with the regenerated catalyst. The desired temperature of the feed inside the reactor is achieved based on the heating of the catalyst in the regenerator. The FCC reaction in the riser is endothermic and the cracking process is occurred in the vapor phase making the feed in the vapor phase. Due to the cracking reactions, the activity of the catalyst is gradually deactivated as a result of coke deposition on the catalyst and increased owing to the cracking reactions, and the reaction is promoted by the catalyst without changing chemically. The catalyst and cracking products will be separated at the stripping process while the hydrocarbons will adsorbed upon the surface of the spent catalyst during the way to the stripper. For stripping and removing the hydrocarbons entrained by catalyst molecules, steam is mostly utilized for this purpose. Product vapor is left the cyclone section, whereas hot product vapor of the reactor goes near to the fractionators, where the hydrocarbon compounds will be condensed and then vaporized in such device. The unstabilized GLN and LG obtained from the top of the main fractionators are sent to the wet gas compressor. The regeneration of the catalyst should be kept constant due to coke (poisoning). In the generator, such issue is taking place, where the activity of the catalyst is restored and providing heat that makes the endothermic reactions of cracking process. The fresh air is coming by blower for the purpose of burning off the coke (consisting of C, H_2, S and N) by air distributor found at the bottom of the regenerator container. The dry gases producing by coke

combustion are passed into cyclones located near the top of the regenerator, while in some operations sends to a carbon monoxide boiler (**Sadeghbeigi, 2000; Kumer, 2012).** The main parts of the FCC unit that have been modeled are:

A) Preheat system
B) Riser
C) Reactor
D) Regenerator

A) Preheat System

The VGO and reduced crude residue produced by atmospheric and vacuum fractionators tower are regarded the main feedstock for the fluid catalytic cracking process. Such feed stocks are heated earlier before going to the reactor, which is carried out via heating system providing the heat required for both fresh and recycled feedstock. Many heat exchangers are employed for this purpose and the temperature required is approximate 260-372 °C. The gas oil includes paraffins, aromatics and naphthenes compounds in addition to some impurities (mainly, S, N) having harmful impact upon the activity of the catalyst. Thus, for the purpose of protecting the pre-treating of the catalyst feed, it is necessary to get rid such impurities before entering to the FCC process to get higher quantity and quality for the products.

B) Riser

All the cracking reactions are carried out in this device (which is considered the major reactor) in endothermic behavior. The contact time in this reactor is reported to be two to ten seconds. The gases generated pass to the fractionators from the top of the reactor, whereas the some liquid product (heavy) and catalyst return in the disengaging section. The oil is separated from the catalyst utilizing the baffles located in the stripping device by steam, which is supplied to the stripping area. The optimal diameter as well as the length of such reactor has observed to be 2 m and 30 to 35 m, respectively **(Fahim et al., 2009; Kumar, 2012)**.

C) Reactor

The previous practice for the implementation of cracking reactions (CR) in the reactor was completely modified by implementing it at the riser section for the purpose of employing the highest efficiency of the catalyst beside temperature in the riser. Previously, no significant efforts have observed to control the processes of the riser, while recently, by using efficient zeolite catalyst leads to enhance the cracking reactions inside the riser. After that, the reactor is then applied to separate both the catalyst and products generated. The improvement of the reactions in the riser is enhanced by an increase in the speed of regenerated catalyst to the required level. In general, the aims of reactor are separating the catalyst deactivated of the cracked vapors, and passing the catalyst used downward through a steam stripper part to the regenerator.

When the hot catalyst meets the feedstock inside the riser, the reactions required are continuously occurred until product vapor is removed from the catalyst in the reactor separator. After that, the products are passed to the fractionators in order to separate the liquids and gases products. The CTO inside the reactor should be kept properly due to ability of changing the product selectivity. The sensible heat of the catalysts can be employed for the CR as well as to vaporize the feedstock **(Gupta and Rao, 2003; Kumar, 2012).**

D) Regenerator

The deactivated catalyst obtained via steam stripper part is sent to the regenerator, where the catalytic activity is maintained (owing to the coke deposited upon the catalyst surface) by using the regeneration process, which is also utilized to supply the heat required to the reactor **(Reza, 2000, Kumar, 2012)**. The air is used for this purpose provided by blowers and the air velocity is kept at high level in the regenerator in order to make the reaction section fluidized in nature and the air is passed to the regenerator via distributor to burn off the large amount of the coke content. The hot catalyst is left the regenerator into a catalyst and the dry gaseous (DG) allow to get out and flowing back to the top section of the regenerator and the fresh catalyst flow is controlled using a slide valve. Two cyclones are used to send the hot DG to the regenerator in order to remove the entrained catalyst from DG. The design and model of the regenerator is selected to burn the coke to CO and CO_2. Nowadays, the modern design of such unit is aimed to convert C into CO_2 with minimum capital cost and coke content **(Han and Chung, 2001a, Kumar, 2012)**.

Figure 1 shows the typical UOP fluidized catalytic cracking unit.

3. Mathematical Model of Riser

The modeling of riser reactor includes the selection of kinetic model and hydrodynamic model. The most important factor considered in the modeling is the balance of simplicity and preciseness. Mathematical model is a set of ordinary algebraic and differential equations related to mass and energy balance and the physical properties of a system. The basic mathematical model for a chemical reaction rate should take into consideration the rate of mass and heat transfer together with the kinetic equation. Mathematic model of such reactor involves the feedstock vaporization, the riser as well as the stripper column and the modelling process is based on an adiabatic plug-flow (PF) reactor with a six-lump kinetics model. The lumped model used in this work is presented in Figure 2 and consisting of vacuum gas oil (VGO), gasoline (GLN), light cycle oil (LCO), liquefied petroleum gas (LPG), dry gas (DG) and coke (CK**).**The complexity of reversible catalyst deactivation by coking during catalytic cracking makes the problem very difficult to analyze from fundamental points of view. Thus in this work, the approach considered is that the pore blockage (external coke deposition) disables higher number of active sites than the site coverage (internal coke deposition), thus the former should be included as the major point of backward catalyst deactivation owing to form the coke **(Shuyan et al., 2008)**. This pore blockage is found because of growth in the coke, where the out surface of the catalyst has mainly deactivated by nickel upon the catalyst matrix. As reaction proceeds, the activity of the catalyst is decreasing by increasing in the coke generated on the catalyst leading to reduce the active sites of the catalyst and the effective rate of the reaction is reduced as a result of reducing the effective diffusivity of the reactants. Therefore, it is an important to take into account the effectiveness factor (η) of the catalyst **(Fernandes et al., 2007)**.

3.1 Mass Balance of Riser

The riser is a PFR under adiabatic conditions. To estimate the concentration behavior for each lump along the reactor, the following equation is used for this purpose **(Weekman, 1968)** as follows**:**

$$\frac{1}{\rho_v}.\frac{\partial(\rho_v.Y_i)}{\partial t_c}\Big|_z + U_V.\frac{\partial Y_i}{\partial z}\Big|_{t_c} = R_i \qquad \textbf{(1)}$$

As reported by **Ali and Rohani (1997),** the left term $\frac{1}{\rho_v}.\frac{\partial(\rho_v.y_i)}{\partial t_c}\Big|_z$ is ignored. Thus the above equation can be written to be:

$$U_V.\frac{\partial y_i}{\partial z}\Big|_{t_c} = R_i \quad \textbf{(2)}$$

$$R_i = \sum_j \hat{r}_{ji} - \sum_j \hat{r}_{ij} \quad \textbf{(3)}$$

$$\hat{r}_{ij} = K_{ij}\, A_i\, \varphi\, \eta\, y_i^{n_{ij}} \mathrm{CTO} \quad \textbf{(4)}$$

3.2 Rate Constant

Reaction rate constant can be described by Arrhenius equation as follow:

$$K_{ij} = a_{ij} exp\,(\frac{-E}{RT}) \quad \textbf{(5)}$$

The sophisticated lumps model has recently been modified to include the characterization of the catalyst and the feed stock. Such modification is proposed to calculate the kinetic constants as a function of API gravity for the lumps**.**

$$K_{ij} = a_{ij} \quad \textbf{(6)}$$

Calculation of such kinetic constant of cracking process related to the conversion of vacuum gas oil to DG is then modified to include the sulfur content in the feed:

$$K_{ij} = a_{ij} S^{b_{ij}} \quad \textbf{(7)}$$

The mobil metal index, M_{MI} (consider for metals impact, namely vanadium and nickel) related to a_i above is taken into account within the rate equations **(Sadeghbeigi, 2000)**:

$$\mathrm{M_{MI}} = \mathrm{N_i} + \frac{\mathrm{V}}{4} \quad \textbf{(8)}$$

3.3 Catalyst Deactivation

The catalyst deactivation function (φ) occurs owing to coke generated on the catalyst. Generally, there are two paths of its representation: the first is based on the residence time upon the catalyst, and the second is dependent upon the coke content. In this study, a single deactivation function based on the catalyst coke content has been formulated to take into account the regenerator efficiency as follows:

$$\frac{d\varphi}{dY_{ck}} = -\alpha_{Yck} \quad \textbf{(9)}$$

Integration eq (9) will give:

$$\varphi = [1 + (d-1) * \alpha_{Yck} Y_{ck}]^{\frac{1}{1-d}} \quad \textbf{(10)}$$

3.4 Effectiveness Factor

The effectiveness factor (ɳ) is based on a Thiele modulus (Φ) as presented in the following relation applied for sphere particles **(Froment et al., 1990, Jarullah et al., 2011a)**:

$$\eta \frac{3(\Phi coth\Phi - 1)}{\Phi^2} \quad \textbf{(11)}$$

The generalized Thiele modulus (Φ)

$$\Phi \frac{V_p}{S_p} = \sqrt{\left(\frac{n+1}{2}\right) \frac{K_{ij}(y_{VGO})^{n-1}\rho_p}{D_{ei}}} \quad \textbf{(12)}$$

The Particle density (ρ_p), can estimating using the following simple relation as follow:

$$\rho_p = \frac{\rho_{cat}}{1-\epsilon_B} \quad \textbf{(13)}$$

The Bed porosity (ϵB) of the catalyst can be estimated for undiluted sphere packed catalyst from the following equation **(Forment et al., 1990; Jarullah et al., 2012) :**

$$\epsilon_B = 0.38 + 0.073\left(1 + \frac{\left(\frac{d_t}{d_{pe}} - 2\right)^2}{\left(\frac{d_t}{d_{pe}}\right)^2}\right) \quad \textbf{(14)}$$

For spherical shape of particle, the external volume (V_p) and the surface area (S_p) of particle can be calculated as shown below:

$$V_p = \frac{4}{3}\pi\left(r_p^3\right) \quad \textbf{(15)}$$

$$S_p = 4\,\pi\left(r_p^2\right) \quad \textbf{(16)}$$

The effective diffusivity (D_{ei}), where the porosity and tortuosity of the pore matrix in the particle should be taken into account in the model **(Wang et al., 2009; Nawaf et al., 2015) .**

$$D_{ei} = \frac{\epsilon_s}{\tau} \frac{1}{\frac{1}{D_{mi}} + \frac{1}{D_{ki}}} \quad \textbf{(17)}$$

The effective diffusivity **(Wang et al., 2009)** which consists of two diffusion contributions :Knudsen diffusivity (D_{ki}) and molecular diffusivity (D_{mi}). D_{ki} is evaluated as shown below **(Mederos, 2009; Nawaf et al., 2015a):**

$$D_{ki} = 9700\, r_g \left(\frac{T}{MW_{VGO}}\right)^{0.5} \quad \textbf{(18)}$$

Mean pore radius (rg), can be estimated by **(Papayannakos and Georgiou, 1988; Jarullah et al., 2013)**

$$r_g = 2\frac{V_g}{S_g} \quad \textbf{(19)}$$

While the D_{mi} is calculated by a **Tyn-Calus equation (Jarullah, 2011; Mohammed et al., 2016)**

$$D_{mi} = 8.93 \times 10^{-8} \frac{v_L^{0.267} T}{v_{VGO}^{0.433} \mu_L} \quad \textbf{(20)}$$

The molar volume of VGO is evaluated by the following relation:

$$v_{VGO} = 0.285\ (v_{cVGO})^{1.048} \quad \textbf{(21)}$$

The critical specific volume vacuum gas oil is calculated by a **Riazi – Daubert** equation **(Ahmed, 1989)**:

$$v_{cL} = (7.5214\ \times 10^{-3} (T_{meABP})^{0.2896} (\rho_{15.6})^{-0.7666}) MW_L \quad \textbf{(22)}$$

The mean average boiling points can be estimated as follows (**Han and Chung, 2001b; Jarullah et al., 2015)**:

$$T_{meABP} = -0.5556\ exp[-0.9440 - 0.0080(1.8\, T_{VABP} - 491.76)^{0.6667} + 2.9972(Sl)^{0.3333}] \quad \textbf{(23)}$$

Where:

$$T_{VABP} = 0.2(T_{10} + T_{30} + T_{50} + T_{70} + T_{90}) \quad \textbf{(24)}$$

$$(Sl) = 0.0225(T_{90} - T_{10}) \quad \textbf{(25)}$$

3.5 Riser Hydrodynamic

When the vaporization process of the feed is completed, the catalyst, coke and gases are left. Depending on the mathematical modeling, the next relation reported by **Patience et al. (1992)** to estimate the slip factor (defined as a ratio between velocity of the average solids and the interstitial gas) is used:

$$\psi = \frac{u_g}{u_p} = \frac{u_o}{\varepsilon_g u_p} = 1 + \frac{5.6}{F_r} + 0.47 F_{r_t}^{0.41} \quad \textbf{(26)}$$

$$F_r = \frac{u_o}{\sqrt{gD}} \quad \textbf{(27)}$$

$$F_{rt} = \frac{u_t}{\sqrt{gD}} \quad \textbf{(28)}$$

The superficial gas velocity is evaluated utilizing the following correlation:

$$u_o = \frac{F_g}{A\, \rho_g} \quad \textbf{(29)}$$

The average particle velocity is calculated as follows **(Ahari et al., 2008)**:

$$u_o = \frac{F_c}{\rho_{cat}(1-\varepsilon_g)} \quad \textbf{(30)}$$

Combining equations 26, 27 and 28, the average void fraction of the gas phase is calculated as follows:

$$\varepsilon_g = \frac{\rho_{cat} F_g}{\rho_g F_c \psi + \rho_{cat} F_g} \quad \textbf{(31)}$$

Hence, the velocity of the vapor (u_g) and solid (u_p) is determined as:

$$u_g = \frac{u_o}{\varepsilon_g} \quad \textbf{(32)}$$

$$u_p = \frac{u_g}{\psi} \quad \textbf{(33)}$$

In order to calculate the particle terminal velocity, many correlations were used in the literatures. In general, the terminal velocity is generally estimated for three areas: Stokes (SK), Intermediate (IN) and Newton (N) areas and it is classified according to Archimedes numbers (*Ar*). Where, *Ar* is reported to be < 32.9, 32.9 to 106.5 and > 106.5 for SK, IN and N, respectively. In this work, (equation 35) for intermediate regime has been employed for calculating Reynolds number based on particle terminal velocity **(Svoboda et al., 2009; Rabinovich and Kalman, 2011).**

$$A_r = \frac{\rho_g(\rho_{cat}-\rho_g)\, g d_p^3}{\mu_g^2} \quad \textbf{(34)}$$

$$Re_t = \frac{A_r}{18+(2.3348-1.7439\, sph){A_r}^{0.5}} \quad \textbf{(35)}$$

$$u_t = \frac{Re_t \mu_g}{\rho_g d_p} \quad \textbf{(36)}$$

The vapor phase density is calculated by the following equation:

$$\rho_g = \frac{PMW_g}{RT} \quad \textbf{(37)}$$

The average vapor phase molecular weight expressed **(Ahari et al., 2008)** as:

$$MW_g = \frac{1}{\frac{y_1}{MW_{VGO}}+\frac{y_2}{MW_{LCO}}+\frac{y_3}{MW_{GLN}}+\frac{y_4}{MW_{LPG}}+\frac{y_5}{MW_{DG}}+\frac{y_6}{MW_{CK}}+\frac{y_7}{MW_{H2O}}} \quad \textbf{(38)}$$

Substituting the equations related to the reaction rate constant and deactivation in the mass balance equation leads to get the general mass equations of the catalytic cracking reactions, which are as follows:

$$\frac{dy_i}{dz} = \frac{1}{\mathrm{U_V}} k_{ij} A_i [1+(d-1)\alpha_{Yck} Y_{ck}]^{-\frac{1}{d-1}} \exp\left(-\frac{E_1}{RT}\right) y_1^{n_1} \eta\, CTO \quad \textbf{(39)}$$

Finally, the following differential equations are used to describe the FCC model for each lump

- $r_{VGO\rightarrow LCO}$

$$\frac{dy_1}{dz} = \frac{1}{\mathrm{U_V}} k_1 M_{MI}^{-0.43} API^{-1.5} [1+(d1)\alpha_{Yck} Y_{ck}]^{-\frac{1}{d-1}} \exp\left(-\frac{E_1}{RT}\right) y_1^{n_1} \eta\, CTO \quad \textbf{(40)}$$

- $r_{VGO\rightarrow CLN}$

$$\frac{dy_1}{dz} = \frac{1}{\mathrm{U_V}} k_2 M_{MI}^{-0.42} API^{1.62} [1+(d-1)\alpha_{Yck} Y_{ck}]^{-\frac{1}{d-1}} exp\left(-\frac{E_2}{RT}\right) y_1^{n_1} \eta\, CTO \quad \textbf{(41)}$$

- $r_{VGO\rightarrow LPG}$

$$\frac{dy_1}{dz} = \frac{1}{U_V} k_3 M_{MI}^{-0.52} API^{1.7} [1+(d-1)\alpha_{Yck} Y_{ck}]^{-\frac{1}{d-1}} exp\left(-\frac{E_3}{RT}\right) y_1^{n_1} \eta\, CTO \quad \textbf{(42)}$$

$r_{VGO\rightarrow DG}$

$$\frac{dy_1}{dz} = \frac{1}{U_V} k_4 M_{MI}^{-0.22} S^{0.14} [1+(d-1)\alpha_{Yck} Y_{ck}]^{-\frac{1}{d-1}} exp\left(-\frac{E_4}{RT}\right) y_1^{n_1} \eta\, CTO \quad \textbf{(43)}$$

❖ $r_{VGO \rightarrow CK}$

$$\frac{dy_1}{dz} = \frac{1}{U_V} k_5 M_{MI}^{-0.43} [1 + (d-1)\alpha_{Yck} Y_{ck}]^{-\frac{1}{d-1}} exp\left(-\frac{E_5}{RT}\right) y_1^{n_1} \eta\, CTO \quad \textbf{(44)}$$

❖ $r_{LCO \rightarrow GLN}$

$$\frac{dy_2}{dz} = \frac{1}{U_V} k_6 M_{MI}^{-0.42} [1 + (d-1)\alpha_{Yck} Y_{ck}]^{-\frac{1}{d-1}} exp\left(-\frac{E_6}{RT}\right) y_2^{n_2} \eta\, CTO \quad \textbf{(45)}$$

❖ $r_{LCO \rightarrow CK}$

$$\frac{dy_2}{dz} = \frac{1}{U_V} k_7 M_{MI}^{-0.42} [1 + (d-1)\alpha_{Yck} Y_{ck}]^{-\frac{1}{d-1}}]\, exp\left(-\frac{E_7}{RT}\right) y_2^{n_2} \eta\, CTO \quad \textbf{(46)}$$

❖ $r_{GLN \rightarrow LPG}$

$$\frac{dy_3}{dz} = \frac{1}{U_V} k_8 M_{MI}^{-0.52} [1 + (d-1)\alpha_{Yck} Y_{ck}]^{-\frac{1}{d-1}} exp\left(-\frac{E_8}{RT}\right) y_3^{n_3} \eta\, CTO \quad \textbf{(47)}$$

❖ $r_{GLN \rightarrow DG}$

$$\frac{dy_3}{dz} = \frac{1}{U_V} k_9 M_{MI}^{-0.22} [1 + (d-1)\alpha_{Yck} Y_{ck}]^{-\frac{1}{d-1}} exp\left(-\frac{E_9}{RT}\right) y_3^{n_3} \eta\, CTO \quad \textbf{(48)}$$

❖ $r_{LPG \rightarrow DG}$

$$\frac{dy_4}{dz} = \frac{1}{U_V} k_{10} M_{MI}^{-0.22} [1 + (d-1)\alpha_{Yck} Y_{ck}]^{-\frac{1}{d-1}} exp\left(-\frac{E_{10}}{RT}\right) y_4^{n_4} \eta CTO \quad \textbf{(49)}$$

3.6 Octane Number

The gasoline octane number can be estimated using the following equation*:*

$$octane\ number\ = \frac{MON+RON}{2} \quad \textbf{(50)}$$

The following equations are employed to calculated the motor octane number (MON) and the research octane number (RON) **(Ellis et al., 1998):**

$$MON = 72.5\ +\ 0.05(\mathrm{T} - 900)\ +\ 0.17(\mathrm{cv} - 0.55) \quad \textbf{(51)}$$

$$RON = 1.29\mathrm{MON}\ +\ 12.06 \quad \textbf{(52)}$$

3.7 Stripper Model

The stripper model equations are introduced as**:**

$$T_{sc} = T_R - \Delta T_{sc} \quad \textbf{(53)}$$

$$F_{sc} = F_{rge} + C_{sc} F_{rge} \quad \textbf{(54)}$$

3.8 Regenerator Model

In the regenerator, the cock generated on the catalyst particles having carbon (C) and H_2, where all the H_2 converts to vapor whereas the carbon converts to either carbon monoxide dioxide. The regenerator model is proposed to have two zones: the Dense bed and the Dilute phase. Based on the literature, the following points are reported: **(Krishna and Parkin, 1985; Mcfarlane et al., 1993; Kasat et al., 2002; Dave and Saraf, 2003):**

- ❖ The gases follow PF mode through the bed and are thermal equilibrium with surrounding bed in nature.
- ❖ Very well mixing for catalyst in dense bed and isothermal mode with uniform C on catalyst.
- ❖ The mass transfer resistance from gas phase to solid phase can be ignored.
- ❖ The specific heat capacity of gas and compound are constant.
- ❖ The cyclones return all entrained catalyst.

The following reactions are reported to be in the regenerator:

$$C + \frac{1}{2}O_2 \overset{K_1}{\rightarrow} CO \quad \textbf{(55)}$$

$$C + O_2 \overset{K_2}{\rightarrow} CO_2 \quad \textbf{(56)}$$

$$CO + \frac{1}{2}O_2 \overset{K_{3c}}{\longrightarrow} CO_2 \quad \textbf{(57)}$$

$$CO + \frac{1}{2}O_2 \overset{K_{3h}}{\longrightarrow} CO_2 \quad \textbf{(58)}$$

$$H_2 + \frac{1}{2}O_2 \overset{K_4}{\rightarrow} H_2O \quad \textbf{(59)}$$

The coke combustion reaction above is expressed given by equation 57 and 56, which are proportional to the coke on regenerated catalyst (C_{rge}), and to partial pressure of oxygen (P_{O2}). The combustion reaction of carbon monoxide equations (equation 57 (Heterogeneous CO combustion) and 58 (Homogeneous CO combustion)) are proportional to (P_{O2}) as well as the partial pressure of CO inside the regenerator (P_{CO}). These reaction rate equations are:

Rate of reaction 1

$$r_1 = (1-\varepsilon)\rho_{cat}k_1\frac{C_{rge}}{MW_{ck}}P_{O2} = (1-\varepsilon)\rho_{cat}k_1\frac{C_{rge}f_{O2}}{MW_{ck}f_{TOt}}P_{rge} \quad \textbf{(60)}$$

Rate of reaction 2

$$r_2 = (1-\varepsilon)\rho_{cat}k_2\frac{C_{rge}}{MW_{ck}}P_{O2} = (1-\varepsilon)\rho_{cat}k_2\frac{C_{rge}f_{O2}}{MW_{ck}f_{TOt}}P_{rge} \quad \textbf{(61)}$$

Rate of reaction 2

$$r_3 = K_3P_{O2}P_{CO} = \left(X_{pt}(1-\varepsilon)K_{3c}\rho_{cat} + \varepsilon K_{3h}\right)\frac{f_{O2}f_{CO}}{{f_{TOt}}^2}{P_{rge}}^2 \quad \textbf{(62)}$$

$$C_{rge} = \frac{F_{sc}C_{sc}(1-C_H)-(f_{co}+f_{co2})MW_{ck}}{F_{rge}(1-C_H)} \quad \textbf{(63)}$$

$$\varepsilon = \frac{0.305u_1+1}{0.305u_1+2} \quad \textbf{(64)}$$

$$u = \frac{F_{air}}{\rho_g A_{rge}} \quad \textbf{(65)}$$

$$\rho_g = \frac{P_{rge}}{RT_{rge}} \quad \textbf{(66)}$$

Reaction constant depends on the temperature and are calculate based on Arrhenius equation **(Fogler, 1999)**

$$\frac{CO}{CO_2} = \frac{K_1}{K_2} = \beta_c = \beta_{co}exp\left(\frac{-E_\beta}{RT}\right) \quad \textbf{(67)}$$

K_c is overall coke combustion rate and

$$K_c = K_1 + K_2 = k_{co} exp\left(\frac{-E_c}{RT}\right) \quad \textbf{(68)}$$

Where:

$$K_1 = \frac{\beta_c K_c}{\beta_c + 1} = \frac{\beta_c k_{co} exp\left(\frac{-E_c}{RT}\right)}{\beta_c + 1} \quad \textbf{(69)}$$

$$K_2 = \frac{K_c}{\beta_c + 1} = \frac{k_{co} exp\left(\frac{-E_c}{RT}\right)}{\beta_c + 1} \quad \textbf{(70)}$$

3.8.1 Dense Bed Modeling

The used catalyst obtained from the reactor is entered to the dense bed where coke is burned-off in by air to carbon monoxide, carbon dioxide and vapor. The H_2 oxidized is proposed to be completed, thus the amount of O_2 available is what is left over after the H_2 combustion reaction (**Dave, 2001)**.

Differential Balances of Dense Bed:

The following mass balance and heat balance are employed for the dense bed:

Material Balance of dense bed:

$$\frac{df_{O2}}{dz} = -A_{rge}\left(\frac{r_1}{2} + r_2 + \frac{r_3}{2}\right) \quad \textbf{(71)}$$

$$\frac{df_{co}}{dz} = -A_{rge}(r_3 - r_1) \quad \textbf{(72)}$$

$$\frac{df_{co2}}{dz} = -A_{rge}(r_2 + r_3) \quad \textbf{(73)}$$

Energy Balance of dense bed:

$$\frac{dT_{rge}}{dz} = 0 \quad \textbf{(74)}$$

Energy balance across the regenerator dense bed is given as follows:

$$Q_c + Q_H + Q_{air} + Q_{sc} + Q_{ent} = Q_{rge} + Q_{sg} + Q_{loss} \quad \textbf{(75)}$$

$$Q_c = f_{co} H_{co} + f_{co2} H_{co2} \quad \textbf{(76)}$$

$$Q_H = f_{H2O} H_{H2O} \quad \textbf{(77)}$$

$$Q_{air} = F_{air} C_{Pair}(T_{air} - T_{bace}) \quad \textbf{(78)}$$

$$Q_{sc} = F_{sc} C_{Pc}(T_{sc} - T_{bace}) \quad \textbf{(79)}$$

$$Q_{ent} = F_{ent} C_{Pc}(T_{dil} - T_{bace}) \quad \textbf{(80)}$$

$$Q_{rgc} = F_{rge}C_{Pc}\left(T_{rge} - T_{bace}\right) \quad \textbf{(81)}$$

$$Q_{sg} = f_{co2}C_{pco2} + f_{co}C_{pco} + f_{N2}C_{pN2} + f_{o2}C_{po2} + f_{H2O}\mathrm{C_{pH2O}} \quad \textbf{(82)}$$

The final expression related to the temperature of the dense bed is

$$T_{rge} = T_{base} + \left\{\frac{Q_C + Q_{H2O} + Q_{air} + Q_{sc} - Q_{loss,rge}}{Q_{sg}}\right\} \quad \textbf{(83)}$$

3.8.2 Dilute Phase Modeling

Converting carbon monoxide to carbon dioxide is regarded the main chemical reaction in the dilute. Thus, both carbon concentration and T are varied based on the height in the dilute phase. Mass and heat balance equation in such area are expressed as follows **(Dave, 2001)**.

Material Balance dilute Phase:

$$\frac{df_{O2}}{dz} = -A_{rge}\left(\frac{r_1}{2} + r_2 + \frac{r_3}{2}\right) \quad \textbf{(84)}$$

$$\frac{df_{co}}{dz} = -A_{rge}(r_3] - r_1) \quad \textbf{(85)}$$

$$\frac{df_{co2}}{dz} = -A_{rge}(r_2 + r_3) \quad \textbf{(86)}$$

$$\frac{df_c}{dz} = -A_{rge}(r_1 + r_2) \quad \textbf{(87)}$$

Energy Balance of dilute Phase:

$$\frac{dT_{dil}}{dz} = \frac{1}{f_{Tot}C_{PTot}}H_{co}\frac{df_{co}}{dz} + H_{co2}\frac{df_{co2}}{dz} \quad \textbf{(88)}$$

$$C_{PTot} = \frac{C_{PN2}f_{N2} + f_{o2}C_{Po2} + f_{co}C_{Pco} + f_{co2}C_{Pco2} + C_{PH2O} + F_{ent}C_{Pc}}{f_{Tot}} \quad \textbf{(89)}$$

The overall process model results in a set of differential and algebraic equations (DAEs).

4. The Experimental Data

To develop first the kinetic models of the process and then the overall FCC process model, the experimental data from **Xiong et al., (2015)** are used. A brief description about the materials, apparatus (as shown in Figure 3 (**Xiong et al., (2015))** and experimental procedure used by **Xiong et al. (2015**) is given below for the convenience of the readers:

- The reaction take place in a plug flow reactor (specifications in Table 1)
  New catalyst is charged before starting with a new experiment.
- The CTO is maintained via keeping the catalyst (which is the zeolite) loading amount and the feedstock (which is the VGO) rate constant.

- Steam flow rate is remained constant and is passed continuously over the catalyst bed with different T for 20 minutes with a new experiment.
- The condensed liquid products are obtained by the container while the gasses will be received in a gas receiving bottle.
- The stripper is used to separate the used catalyst steam for 30 min for the purpose of recovering entrapped hydrocarbons and the coke is burned off with O_2 by heating the catalyst at 953 K leading to convert the carbon monoxide to carbon dioxide.

5. Estimation of Kinetic Parameters of the Model

In efferent areas of science and engineering, kinetic parameters evaluation is important due to several physical and chemical operations stated by a set of relations with unknown factors. Estimation of kinetic parameters is a significant and not a simple step in the improvement of models but can be facilitated by utilizing model based techniques and experimental data. Minimizing the errors between experimental results and predicted data are required when adequate estimation of kinetic parameters is needed. In this work, a non-linear regression method is utilized to determine the reaction orders of VGO (n_1), LGO (n_2), gasoline (n_3) and LPG (n_4), activation energy (E_{ij}) and pre-exponential factor (A_{ij}) for each reaction.

The minimization of the sum of squared errors (SSE) between the experimental concentrations of product (y_i^{exp}) and predicted (y_i^{pred}) is utilized for parameter estimation and the objective function (OBJ), which is minimized can be written as follows:

$$OBJ = \sum_{n=1}^{N_t} \left(y_i^{exp} - y_i^{pred}\right)^2 \quad \textbf{(90)}$$

5.1 Optimization Problem Formulation for Parameter Estimation of FCC (OP1):

The parameter estimation problem formulation can be stated as follows:

Given	The reactor characterization, the catalyst, the VGO, the process conditions
Optimize	The reaction orders of FCC reactions (n_1,n_2,n_3,n_4), reaction rate constants (k) at various temperatures
So as to minimize	The sum of square errors (*SSE*)
Subject to	Constraints on the conversion and linear bounds on all optimization variables

Mathematically, the problem is stated as:

Min SSE
$n_1, n_2, n_3, n_4, A_i, E_i$ *(i=1-10)*

s.t. f (z, x(z), (x`(t), u(z), v)=0 ,[z_o , z_f] [model, equality constraint]

$n_1{}^L \le n \le n_1^U$ [inequality constrain

$n_2{}^L \le n \le n_2^U$ [inequality constraint]

$n_3{}^L \le n \le n_3^U$ [inequality constraint]

$$n_4{}^L \le n \le n_4^U \qquad \text{[inequality constraint]}$$

$$A_i{}^L \le A \le A_i^U \qquad \text{[inequality constraint]}$$

$$E_i{}^L \le E \le E_i^U \qquad \text{[inequality constraint]}$$

Where: f (z, g(z), g˜(z), a(z), p)=0 represents the process models that presented in section 3. *Z* is the length of the reactor bed (independent variable), a(z) is the decision variables (n_1, n_2, n_3, n_4 ,E_i, A_i), g(z) refers to the differential and algebraic variables (y_{VGO}, y_{LCO},….), g˜(z) refers to the derivative of differential variables with respect to bed length of reactor such as ($\frac{dy_{vgo}}{dz}$, $\frac{dy_{GLN}}{dz}$…..) and p is length (independent constants parameters) or design variables such as (*R*, …). [z_0, z_f], is the length interval of interest.

The solution way for the optimization utilizing gPROMS is by two-way approach known as feasible path approach.

- The first way is to perform the simulation for converging all the equality constraints (described by ***f***) and satisfying the inequality constraints.
- The second way is performing the optimization (to update the values of the decision variables such as the kinetic parameters).

The optimization problem is posed as a NonLinear Programming (NLP) problem and is solved using a Successive Quadratic Programming(SQP) method with in gPROMS software.

6. Scale Up of Fluidized Catalytic Cracking Reactor

Optimal operating conditions based on maximum conversion and octane number, and minimum coke content of the catalyst regenerated of an industrial scale FCC is investigated here, which was not considered in the experimental system. Here the goal is minimizing the cost and maximizing the profitability of the scaled up process**.**

6.1 Energy Balance in Riser

The heat supplied to the reactor is coming from the regenerator via hot circulating catalyst **(Stratiev and Dinkov, 2007)**. For heat balance, the risers are regarded as adiabatic PFRs and the resistance among gases and solids are negligible. The enthalpy of cracking reactions related to vacuum gas oil cracked represents the overall energy consumed via endothermic CRs and both solids and gases having the same T owing to pseudo-homogeneity for the heat balance, both gas and solids share the same temperature **(Das et al., 2003).** The temperature profile along riser can be estimated utilizing the following energy balance equation **(Fernandes et al., 2012)**:

$$\frac{dT_{RS}}{dz} = \frac{\varepsilon_c \Delta H_{crk} r_{VGO} \Omega_{RS}}{F_g Cp_g + F_c Cp_c} \qquad \textbf{(91)}$$

The following polynomial equation expresses the cracking enthalpy to the riser reactor temperature:

$$\Delta \mathrm{H_{crk}} = a_{\Delta H} T_{RS}^2 + b_{\Delta H} T_{RS} + c_{\Delta H} \qquad \textbf{(92)}$$

Where: $a_{\Delta H}$,$b_{\Delta H}$ and $c_{\Delta H}$ the model parameters

$$Cp_g = \mathrm{a} + \mathrm{bT} + \mathrm{cT}^2 \quad \textbf{(93)}$$

6.2 Optimization of Operating Conditions (OP2):

The process conversion mainly depends on the operating conditions and it is necessary to find the optimal operating conditions which will enable high conversion with high octane number. Many of process variables affect the feedstock conversion. In previous studies, it has been observed that the maximum conversion obtained is about 85% **(Ancheyta and Sotelo, 2000)**,while the maximum octane number reported is about 91%**(Watanabe et al., 2010).**In this study, one of the goals is to achieve higher conversion and octane number than those reported in the literatures.

6.2.1 Optimization Problem Formulation (OP2)

The optimization problem can be stated as:

Given	Length of the reactor (L), the diameter of the reactor (D) and reaction orders (n_1,n_2,n_3,n_4), A_{ij}, E_{ij}
Optimize	reaction temperature (TR), CTO, WHSV
So as to maximize	Conversion function (CV)
Subjected to	Process constraints and linear bounds on all decision variables

Mathematically, the optimization problem can be written as:

Max CV

WHSV, TR, CTO

s.*t*	$f(x(z), u(z), v) = 0$	(model equation, equality constraint)
	$\mathrm{WHSV}^{\mathrm{L}} \leq \mathrm{WHSV} \leq \mathrm{WHSV}^{\mathrm{U}}$	(Inequality constraints)
	$T_{\mathrm{R}}^{\mathrm{L}} \leq \mathrm{T_R} \leq \mathrm{T}_{\mathrm{R}}^{\mathrm{U}}$	(Inequality constraints)
	$\mathrm{CTO}^{\mathrm{L}} \leq \mathrm{CTO} \leq \mathrm{CTO}^{\mathrm{U}}$	(Inequality constraints)
	$CV > CV^*$	(Inequality constraints)

Where, * is the target value.

6.3 Minimum Coke Content of the Regenerated Catalyst (OP3)

As mentioned previously, the cock will be generated upon the catalyst during CRs and such spent catalyst will be regenerated inside the regenerator in order to return it to the reactions area (**Praveen and Shishir, 2009)**. In previous studies related to the coke content, the minimum coke content in regenerated catalyst is reported to be 0.002% **(Han and Chung, 2001b).**Thus, another challenge is to achieve coke content lower than those reported in the literature.

6.3.1 Optimization Problem Formulation For Minimum Coke Content (OP3)

In regenerator model, minimize the coke content on the regenerated catalyst is used here utilizing the following objective function:

$$W = C_{rge} \quad \textbf{(94)}$$

The optimization problem formulation can be stated as follows:

Given	Reactor configuration, kinetic parameters, F_c , C_{sc}, CTO and T_{RS}
Optimize	Air flow rate, coke on regenerated catalyst, regenerator temperature
So as to minimize	W
Subjected to	Process constraints and linear bounds on all decision variables (mentioned above).

Mathematically, the optimization problem can be written as:

Min W

F_{air}

s.*t* $f(x(z), u(z), v) = 0$ (model equation, equality constraint)

$F_{air}^{L} \leq F_{air} \leq F_{air}^{U}$ (Inequality constraints)

$T_{reg}^{L} \leq T_{reg} \leq T_{reg}^{U}$ (Inequality constraints)

$W \geq 0$ (Inequality constraints)

7. Results and Discussions

7.1. The Kinetic Parameters Estimation

The values of constant parameters used to simulate the mathematical model are given in Table 2 and 3. The activation energy (E_i), pre-exponential factor (A_i) and reactions orders of (n_i) have been determined simultaneously by solving optimization problem *OP1* and are presented in Table 4. The values of the activation energy (E_i) and pre-exponential factor (A_i) applied to find the concentrations of the lumps gave error less than 5% among all results (as shown in Figures 4 – 9). The optimal value of the order of vacuum gas oil, light cycle oil, gasoline and liquefied petroleum gases concentration (n_i) are estimated to be (0.925367,1 ,0.999785 ,0.999413) respectively. A wide range of values of activation energy and pre-exponential factor have been reported in literatures and such parameters were within the range reported in the public domain **(Ancheyta and Sotelo, 2000; Fernandes et al., 2007; Fernandes et al., 2008; Xiong et al., 2015)**.

7.2 Effect of Operating Variables on Vacuum Gas Oil Conversion

The effect of each operating variables upon the vacuum gas oil conversion can be summarized as follows:

- Reaction temperature: a set of experiments (taken from literature) were carried out at various temperatures (460, 510 and 540℃) while keeping the others parameters constants (WHSV=15 hr^{-1}, CTO=6).
- Catalyst to oil ratio (CTO): different CTO (4, 7 and 10) have been tested to show the effect of catalyst to oil ratio upon the vacuum gas oil conversion, keeping others parameters constant (temperature = 490 ℃ , WHSV=15 hr^{-1}).
- Wight hourly space velocity (WHSV): various runs of weight hourly space velocity (5, 20 and 30 hr^{-1}) were carried out to declare the effect of time contacting between reactants upon the vacuum gas oil conversion. Other parameters were also kept constant (temperature = 490 ℃ , CTO=6).

7.2.1 Effect of Temperature

Figure 4 shows the experimental data and the model prediction on the effect of temperature on VGO conversion (460 to 540 °C) at constant WHSV of 15 and the CTO of 6. Clearly there is a good match between experimental conversion of VGO and model prediction conversion. The conversion of VGO increased and higher conversion of vacuum gas oil IS obtained at higher temperature. This behavior can be attributed to the fact that at high temperature, reaction rate constants are effectively influenced resulting in an increase in vacuum gas oil conversion depending on the Arrhenius equation where the rate constants are a function of reaction temperature (direct proportion) and activation energy (inverse proportion).

Figure 5 shows the product distribution of FCC reaction (both experimental and model predictions) as a function of T at WHSV of 15 and CTO of 6. Again there is a good match between experimental data and predicted results related to the yields of the lumps as shown in this figure. As the temperature increased from 733K to 813K, the yields of DK and LPG has increased with rising in temperature, and that of the light cycle oil (LCO) decreased. While, the yields of gasoline (GLN) increased initially and to decrease thereafter, and the maximum yield is achieved at 773K, and there was slight difference in gasoline yields at 763K and 773K. Also, the yield of coke (CK) was decreased with increasing in temperature below 763K and rapidly increased higher than 763K. Such behavior is explained as follows: an increase in the rate of reactions by increasing the reaction temperature, higher cracking are obtained according to low vaporization impact with low temperature (**Xiong et al., 2015**). Such behavior related to the results above may also be attributed to that an increase in reaction temperature leading to accelerate intermolecular motions giving higher conversion of the reactants to new components, hence enhancing the chemical reaction rate. Better feed vaporization can be obtained at high temperature in addition to reduce the coke content of unvaporized feed compositions by condensation reactions. The diffusion of feed compositions can be enhanced when higher temperature and lower coke is achieved **(Decroocq, 1984; Shuyan et al., 2008).** It has also been observed from this Figure based on the results that the error was less than 5% among all results with high agreement between the predicted and experimental results.

7.2.2 Effect of Catalyst to Oil Ratio (CTO)

Figure 6 shows the conversion of VGO as a function of CTO at the reaction temperature of 763K and the weight hourly space velocity of 15 hr^{-1} (for both experimental and model predictions). Very good match between the experimental and model conversion is observed in this Figure. Increasing in CTO from 4 to 10, the conversion of vacuum gas oil increased. In other words, as the CTO increased, the concentration of the catalyst will increase leading to increase the reaction rate of primary and secondary cracking. Such behavior enhances the total number of molecules cracked on the catalyst surface leading to increase the amount of coke generated on the particles of the catalyst. As well as, increasing the CTO, higher temperature of the reactor riser is obtained as more heat is enhanced in by the hot regenerated catalyst.

Figure 7 shows the product distribution of FCC reaction (both experimental and model predictions) at different CTO ratio, where an increase in CTO, the yields of gasoline (GLN), dry gas (DG), liquefied petroleum gases (LPG) and coke (CK) has increased whereas decreasing in light cycle oil (LCO). Increasing the catalyst to oil ration CTO leads to increase the catalyst active sites concentration that contributes and more reaction rates of cracking reactions are achieved in addition to higher selectivity toward CRs. Thus, a large catalyst to oil ration is more suitable for the production of gasoline.

As can also be seen from this Figure, a good agreement between experimental and predicted results with average absolute error less than 5% among all the results have obtained via employing such modified model.

7.2.3 *Effect of Weight Hourly Space Velocity*

Figure 8 shows the conversion results as a function of weight hourly space velocity at T of 763K and the CTO of 6. As the WHSV increased from 5 to 30 hr^{-1}, the conversion of VGO has decreased and higher weight hourly space velocity gives lower residence time between VGO and catalyst leading to inhibit the THC as a result of reducing the chemical reactions.

Figure 9 illustrates the product distribution of FCC reaction at several WHSV, where the yield of light cycle oil (LCO) increased by increasing in WHSV. Opposite phenomena can be observed with the yields of DG, LPG) and CK (the yields decreased with increasing in WHSV) as a results of decreasing in contact time. While the yield of gasoline increased initially and then decreased, and the maximum yield is obtained at 15 hr^{-1} owing to the above reasons.

It is also noticed from this Figure that the comparison results between the experimental and predicted values showed a very well agreement with an average absolute error less them 5% among all results.

7.3 Optimal Values of Operating Conditions (OP2)

The optimal values of the best operating conditions related to maximum conversion and the octane number is listed in Table 5. Table 6 and 7 show the results obtained from this study and those obtained by last studies related to conversion and the octane number. It has clearly been noticed from these Tables that the new operating conditions obtained via optimization approach gave better results where the highest conversion is found to be 87.61% and highest octane number is found to be 97.57. The gaseous and liquids mass velocities, molecular diffusivity of the compounds, reaction rate constants of FCC process, viscosities and densities of the components are influenced by the reactor temperature and WHSV leading to increase the conversion of such process. Such behavior supports the fact that the TR is very effective to enhance the degree of catalytic conversion.

The WHSV is also an important reaction parameter, which evaluates the reaction severity as well as the FCC efficiency. A decrease in WHSV leads to increase the contact time enhancing the reaction severity**.** Also, the Successive Quadratic Programming (SQP) method used in this work to maximize the process conversion as well as the octane number is better than those applied in last studies (using various approaches to maximize the OBJ getting optimal design of FCC reactor). This solution method utilized here having high accuracy to determine the decision variables of FCC operation in gPROMS package in addition to the high trust for solving such models, which means that this model can be applied with high confident to reactor design, operation and control leading to get higher profit (higher quality (the highest conversion) and quantity (the highest octane number).

7.4 The Optimal Values of the Coke Content in the Regenerated Catalyst (OP3)

It is necessary to take into account the optimal values of the coke content in the regenerated catalyst because of such parameters can effect on the process efficiency, the conversion and the activity of the catalyst. The optimal values of the best operating conditions used in the regenerator model process with the best operation conditions obtained by the last case studies are employed for this purpose. As shown in Table 8, the optimal coke content in the regenerated catalyst of the industrial FCC process is minimized to be 0.000362 wt% based on the optimal flow rate of the air feed to the regenerated catalyst at 0.55 kmol/s and the optimal temperature of the regenerator of 968.58 K, which is regarded one of the goals of this study. Such new results can be attributed to the accuracy of the model studied here under process conditions and constraints, where all the necessary design parameters, reaction rate equations as a function of operating conditions (collected depending on the experimental results, mass and energy balance, hydrodynamic parameters, physiochemical properties in addition to the catalyst activity that ignored in the literature) have taken into considerations here. Such design and kinetic parameters can effect on the process leading to reduce the sensitivity analysis of the process and giving high deviation and as a results the performance and the behavior of the process can not be predicted confidently in addition to the advanced solution method utilized here (SOP (discussed previously)).The comparative results with those obtained by previous studies are listed in are Table 9.

The new results obtained in this study (the highest conversion and octane number, and the lowest coke content in the regenerated catalyst) compared with those reported in the literature can be attributed to the reasons summarized in Table 10.

7.5 The Behavior of the Industrial FCC Reactor

The best kinetics parameters obtained and model developed can now be employed for simulating the behavior of the industrial fluidized catalytic cracking reactor by varying different process operating parameters to gain deeper insight of the process. The product yield profiles have been modeled along the riser height as shown in Figure 10. This Figure shows the chemical reaction is higher at the riser entrance than other where the high gradient of the variables occur. The molecular weight (MW) of gas phase as a function of the riser length is described in Figure 11, where an increase in the amount of light products within this phase leads to decrease the molecular weight. Despite the amount of steam is few compared with the overall gas phase, the model can give good data of MW based on such amount of steam and giving low gas density as a function of MW as stated in Figure 12. The gas phase and solid phase velocities are plotted in Figure 13, where the velocity of the process can be obtained at the higher values of the riser exit with two phases. The slip factor (SF) is shown in the Figure 14, where higher slip factor is observed at the entrance of the riser and the velocities of the gases are bigger than velocities of the particles, and these velocities increased owing to CRs. It accelerates the catalyst velocity resulting decrease in slip factor. The SF values has ranged to be from 1.2 to 4, and 2 is regarded as typical in a industrial fluid catalytic cracking process **(Fernandes et al., 2005a)**.

8. Conclusions

From the present study, the following conclusions can be reported according to the description of such process:

- A new mathematical of FCC unit models for the riser and regenerator were developed. The best kinetic parameter of the FCC unit to predict the performance of catalytic cracking kinetic reaction in reactor in princess catalyst under different operating conditions (temperature (460, 510 and 540℃), WHSV (5, 20 and 30hr^{-1}), CTO (4, 7 and 10) were investigated here. The results obtained were compared with the pilot plant results and a vary good

agreement is observed .The commercial unit results compared with model results indicated that the description of such unit in more accurate compared with those reported in the public domain.

- The best kinetic parameters of this model were estimated via optimization technique using (Non-Linear methods) based on experimental results depending on minimizing the sum of squared error between experimental and predicted results with average absolute error les that 5% among all the results at various conditions
- The reaction orders of vacuccum gas oil, LCO, GLN and LPG have also been evaluated to be 0.925367,1, 0.999785 and 0.999413 respectively.
- The the feedstock conversion is based on the operating conditions, therefore the optimal process conditions (mainly, T, WHSV, and CTO) have studied here for the purpose of getting the highest conversion .The maximum conversion of FCC (87.61 %) with high octane number (97.57) for the process is obtained at 820 K, 2 hr^{-1} and 10 for T, WHSVand CTO respectively.
- The highest conversion and octane number of FCC unit compared with those reported in the literature have obtained.
- The optimal coke content in rgenerated catalyst is 0.000362 wt % (the lowest content in comparison with previous studies).

Nomenclature

A_i	Rate coefficient	(-)
A_r	Archimedes number	(-)
A	Riser ,Regenerator cross section area	(m^2)
API	Density parameter	(-)
a_{ij}	Pre-exponential factor	($cm^3gm\ s^{-1}$)
b_{ij}	Cracking kinetic parameter of the reaction lump i→ j	(-)
c_i	Cracking kinetic parameter for the formation of $lump_i$	(-)
C_r	Reactor cost	$/yr
C_{rge}	Weight fraction of coke on regenerated catalyst	kg of coke/kg of cat
C_{sc}	Weight fraction of coke on spent catalyst	kg of coke/kg of cat
C_H	Weight fraction of hydrogen in coke	kg of H_2/kg of coke
cp_g	Specific heat capacity of vacuum gas oil	j/gm.k
cp_c	Specific heat capacity of catalyst	j/gm.k
cp_{air}	Specific heat capacity of air	k j/kg.k
cp_{co}	Specific heat capacity of carbon monoxide	k j/kg.k
cp_{co_2}	Specific heat capacity of carbon dioxide	k j /kg.k
cp_{o_2}	Specific heat capacity of oxygen	k j /kg.k
cp_{N_2}	Specific heat capacity of Nitrogen	k j /kg.k
$D_{e,vgo}$	Effective diffusivity of vacuum gas oil	cm^2/sec
$D_{m,vgo}$	Molecular diffusivity of gas oil in liquid phase	cm^2/sec
$D_{k,vgo}$	Knudsen diffusivity of vacuum gas oil	cm^2/sec
d_p	Diameter of catalyst particle	cm
d_{pe}	Equivalent particle diameter	cm
d_t	Tube diameter	cm
D	Riser, Regenerator diameter	cm
E_i	Activation energy	k j/kmol
F_g	Vacuum gas oil mass flow rate	kg/sec
F_{cat}	Catalyst mass flow rate	kg/sec

F_r	Frond number	(-)
F_{rt}	Terminal Frond number	(-)
f_i	Molar flow rate of i gas in regenerator	k mol/sec
f_{TOt}	Total gas flow rate at any location in the regenerator	k mol/sec
F_{sc}	Mass flow rate of spent catalyst	kg/sec
F_{sc}	Mass flow rate of regenerated catalyst	kg/sec
H_{co}	Heat of formation of carbon monoxide	k j/k mol
H_{co_2}	Heat of formation of carbon dioxide	k j/k mol
H_{H2O}	Heat of formation of water	k j/k mol
K_{ij}	Cracking kinetic constant of the reaction in riser lump i→ j	cm^3/gm.sec
k_1, k_2, k_3	Reaction rate constant for composition reaction in regenerator	(-)
k_{3c}, k_{3h}		
k_c	Overall rate combustion of coke	(-)
k_{co}	Frequency factor for ith reaction	(-)
L_r	Length of reactor bed	cm
$M\ \&\ S$	Marshal and swift index for cost escalation	(-)
m_w	Mass flow rate of cooling water	gm/esc
M_{MI}	Mobil metal index	ppm
MW_g	Molecular weight of vacuum gas oil	gm/g mole
MW_{LCO}	Molecular weight of light cycle oil	gm/g mole
MW_{GLN}	Molecular weight of gasoline	gm/g mole
MW_{LPG}	Molecular weight of liquefied petroleum gases	gm/g mole
MW_L	Molecular weight of liquid phase	gm/g mole
MW_{DG}	Molecular weight of dry gas	gm/g mole
MW_T	Average vapor phase Molecular weight	gm/g mole
MW_{CK}	Molecular weight of coke	gm/g mole
n_1	Order of vacuum gas oil concentration	(-)
n_2	Order of light cycle oil concentration	(-)
n_3	Order of gasoline concentration	(-)
n_4	Order of concentration of liquefied petroleum gases	(-)
N_i	Nickel content in the equilibrium catalyst	ppm
p_{o_2}	Partial pressure of oxygen	atm
p	Riser ,regenerator pressure	atm
Re_t	Reynolds number	(-)
R_j	rate formation	gm/cm^3.sec
R	Gas constant	j/mole.k
r_{ij}	Rate of reaction lump i→j	gm/cm^3.sec
r_P	Radius of catalyst particle	cm
r_g	Mean pore radius	cm
S_P	Total geometric surface area of catalyst	cm^2
S_g	Specific surface area of particle	cm^2/gm
S	Sulfur content in feed stock	wt%
T_{meABP}	Mean average boiling point	K
T_R	Riser temperature	K
T_{dil}	Temperature of dilute phase at any location	K
T_{rge}	Regenerator temperature	K
T	Temperature of reaction	K
T_{VABP}	Volume average boiling temperature	K
T_{sc}	Temperature of spent catalyst	K

T_{10}, T_{30} T_{50}, T_{70}, T_{90}	ASTM D86 distillation temperature at distilled vol% equal to 10,30,50,70,90, respectively.	K
T_{base}	Base temperature for heat balance calculation	K
u_g	Velocity of gas	m/sec
u_t	The partial terminal velocity	m/sec
u_p	Velocity of solid particle	m/sec
u_o	Superficial gas velocity	m/sec
U_1	Over all heat transfer coefficient for heat exchanger 1 (H.E.1)	$w/m^2.k$
U_2	Over all heat transfer coefficient for heat exchanger 2 (H.E.2)	$w/m^2.k$
U_3	Over all heat transfer coefficient for cooler	$w/m^2.k$
V_P	Total geometric volume of catalyst particle	cm^3
V_g	Total pore volume	cm^3/gm
V_{cat}	Volume of catalyst	cm^3
V	Vanadium content in equilibrium catalyst	ppm
x_{pt}	Relative (catalytic) co combustion rate	(-)
z	Height of riser, regenerator	m

Greek Symbols

β_c	CO/CO_2 ratio at catalyst surface in regenerator	(-)
β_i	Frequency factor	(-)
ε	Void fraction in regenerator at any location	(-)
ε_g	Void fraction of gas phase in riser	(-)
ϵ_B	Porosity	(-)
ϵ_S	Catalyst particle porosity	(-)
ΔH_{crk}	Heat of craking per unit mass ogf gas oil converted	j/kg
ΔT_{sc}	Stripper temperature drop	°C
η_0	Effectiveness factor	(-)
μ_l	Liquid viscosity	pa.sec
μ_g	Gas viscosity	pa.sec
ρ_p	Particle density	gm/cm^3
ρ_c	Catalyst density	gm/cm^3
ρ_g	Gas density	gm/cm^3
φ	Catalyst activity factor	(-)
Φ	Thiele modulus	(-)
Sph	Spericity	(-)
Ω_{RS}	Cross section area of riser	m^2
$\mathfrak{T}$	Tortuosity factor	(-)
v_{cg}	Critical volume of vacuum gas oil	$cm^3/gmole$
v_g	Molar volume of liquid	$cm^3/gmole$
v_l	Molar volume of liquid	$cm^3/gmole$

References

Ahari, J. S., Farshi, A., & Forsat, K. (2008). A mathematical modeling of the riser reactor in industrial FCC unit. *Petroleum and Coal*, *50*(2), 15-24.

Ahmed, T. (1989). Hydrocarbon Phase Behavior, Gulf Pub. *Co., Houston*.

Ali, H., Rohani, S. (1997). Dynamic modeling and simulation of a riser-type fluid catalytic cracking unit. *Chemical engineering & technology*, *20*(2), 118-130.

Ancheyta, J., Sotelo, R. (2000). Estimation of kinetic constants of a five-lump model for fluid catalytic cracking process using simpler sub-models. *Energy & fuels*, *14*(6), 1226-1231.

Chuachuensuk, A., Paengjuntuek, W., Kheawhom, S. Arpornwichanop, A. (2013). A systematic model-based analysis of a downer regenerator in fluid catalytic cracking processes. *Computers & Chemical Engineering*, *49*, 136-145.

Chen, Y. M. (2006). Recent advances in FCC technology. *Powder Technology*, *163*(1), 2-8.

Colorado school of mines, (2016). "Fluidized Catalytic Cracking", http://ebookdock.com/fluidized-catalytic-cracking.html

Das, A. K., Baudrez, E., Marin, G. B., Heynderickx, G. J. (2003). Three-dimensional simulation of a fluid catalytic cracking riser reactor. *Industrial & engineering chemistry research*, *42*(12), 2602-2617.

Dave, D. 2001. Modeling of a fluidized bed catalytic cracker unit. M. Tech Dissertation. Indian Institute of Technology, Kanpur, India.

Dave, D. J., Saraf, D. N. (2003). A Model Suitable for Rating and Optimization of Industrial FCC Units. *Indian Chemical Engineer, Section (A), 45, 7-19.*

Decroocq, D. (1984). Catalytic cracking of heavy petroleum fractions. Editions Techniq.

Ellis, R. C., Li, X., Riggs, J. B. (1998). Modeling and optimization of a model IV fluidized catalytic cracking unit. *AIChE Journal*, *44*(9), 2068-2079.

Fahim, M. A., Al-Sahhaf, T. A., Elkilani, A. (2009). *Fundamentals of petroleum refining*. Elsevier, UK.

Fernandes, J. L., Pinheiro, C. I. C., Oliveira, N., Ribeiro, F. R. (2005). Modeling and Simulation of an Operating Industrial Fluidized Catalytic Cracking (FCC) Riser. In *Book of abstracts and Full Papers CD of the 4th Mercosur Congress on Process Systems Engineering—ENPROMER 2005*, 38.

Fernandes, J., Verstraete, J. J., Pinheiro, C. C., Oliveira, N., Ribeiro, F. R. (2005a). Mechanistic dynamic modelling of an industrial FCC Unit. *Computer Aided Chemical Engineering*, *20*, 589-594.

Fernandes, J. L., Domingues, L. H., Pinheiro, C. I., Oliveira, N. M., Ribeiro, F. R. (2012). Influence of different catalyst deactivation models in a validated simulator of an industrial UOP FCC unit with high-efficiency regenerator. *Fuel*, *97*, 97-108.

Fernandes, J. L., Pinheiro, C. I., Oliveira, N. M., Inverno, J., Ribeiro, F. R. (2008). Model development and validation of an industrial UOP fluid catalytic cracking unit with a high-efficiency regenerator. *Industrial & Engineering Chemistry Research*, *47*(3), 850-866.

Fernandes, J. L., Verstraete, J. J., Pinheiro, C. I., Oliveira, N. M., Ribeiro, F. R. (2007). Dynamic modelling of an industrial R2R FCC unit. *Chemical engineering science*, *62*(4), 1184-1198.

Fogler, H. S. (1999). Elements of chemical reaction engineering. Prentice Hall PTR.

Froment, G. F., Bischoff, K. B., De Wilde, J. (1990). Chemical reactor analysis and design, Wiley New York.

Gary, J. H., & Handwerk, G. E. (1975). Hydrotreating. *Petroleum Refining Technology and Economics (NY: Marcel Dekker, Inc.)*, 114-120.

Gupta, A., Rao, D. S. (2003). Effect of feed atomization on FCC performance: simulation of entire unit. *Chemical Engineering Science*, *58*(20), 4567-4579.

Han, I. S., Chung, C. B. (2001a). Dynamic modeling and simulation of a fluidized catalytic cracking process. Part I: Process modeling. *Chemical Engineering Science*, *56*(5), 1951-1971.

Han, I. S., Chung, C. B. (2001b). Dynamic modeling and simulation of a fluidized catalytic cracking process. Part II: Property estimation and simulation. *Chemical Engineering Science*, *56*(5), 1973-1990.

Han, I.-S., Chung, C. B., Riggs, J. B. (2000). Modeling of a fluidized catalytic cracking process. *Computers & Chemical Engineering*, 24**,** 1681-1687.

James, H., Glenn, E., Mar, J. (2001). Petroleum refining technology and economics. CRC Press, New York.

Jarullah, A. T., Mujtaba, I. M., Wood, A. S. (2011). Kinetic parameter estimation and simulation of trickle-bed reactor for hydrodesulfurization of crude oil. *Chemical Engineering Science*, *66*(5), 859-871.

Jarullah, A.T., Mujtaba, I.M., Alastair, S.W. (2011a). Kinetic model development and simulation of simultaneous hydrodenitrogenation and hydrodemetallization of crude oil in trickle bed reactor. Fuel 90, 2165‑2181.

Jarullah, A.T., Mujtaba, I.M., Alastair, S.W. (2012). Economic Analysis of an Industrial Refining Unit Applied for Hydrotreating of Crude Oil in Trickle Bed Reactor using gPROMS. Computer Aided Process Eng., 30, 625–656.

Jarullah, A.T., Shymaa, A.H., Zina A.H. (2013). Optimal Design of Ammonia Synthesis Reactor. *Tikrit Journal of Eng. Sci.*, 20, 22-31.

Jarullah, A.T., Arkan J.H., Shymaa, A.H. (2015). Optimal Design of Industrial Reactor for Naphtha Thermal Cracking Process. *Diyala Journal of Eng. Sci*., 8, 139-161.

Jin, Y., Zheng, Y., Wei, F. (2002). State of the art review of downer reactors. *Circulating fluidized bed technology VII*, Ottawa:CSCHE,40-60.

Jones, D. S., Pujadó, P. P. (2006). Handbook of petroleum processing, Springer Science & Business Media.

Kasat, R. B., Kunzru, D., Saraf, D., Gupta, S. K. (2002). Multiobjective optimization of industrial FCC units using elitist nondominated sorting genetic algorithm. *Industrial & engineering chemistry research*, 41, 4765-4776.

Krishna, A. S.,, Parkin, E. S. (1985). Modeling the regenerator in commercial fluid catalytic cracking units. *Chem. Eng. Prog.;(United States)*, *81*(4).

Kumar, A. (2012). Effect of Naphtha Yield, overall Conversion and Coke Yield Though Different Operating Variables in FCC Unit using Aspen-Hysys Simulator. Bsc Thesis, National Institute of Technology, Rourkela.

Li, X., Li, C., Yuan, Q., Yang, C., Shan, H., Zhang, J. (2003). Studies on Conversion of FCC Gasoline to Light Olefins and High Octane Number Gasoline with Low Olefin Content. *Prepr. Pap.-Am. Chem. Soc., Div. Fuel Chem*, *48*(2), 910.

Mcfarlane, R. C., Reineman, R. C., Bartee, J. F., Georgakis, C. (1993). Dynamic simulator for a model IV fluid catalytic cracking unit. *Computers & chemical engineering*, 17, 275-300.

Mederos, F. S., Elizaldi, G., Ancheyta, J. (2009). Steady-State and Dynamic Reactor Models for Hydrotreatment of Oil Fractions: A Review. *Catal. Rev*. 51,485−607.

Meyers, R. A. (2004). *Handbook of petroleum refining processes*. McGraw-Hill.

Mohammed, A.E., Jarullah, A.T., Ghani, S.A., Mujtaba, I.M. (2016). Optimal design and operation of an industrial three phase reactor for phenol oxidation. Computers & Chemical Engineering, 94, 257-271

Nawaf, A.T., Saba A.G., Jarullah, A.T., Mujtaba, I.M., (2015). Optimal Design of a Trickle Bed Reactor for Light Fuel Oxidative Desulfurization Based on Experiments and Modeling. Energy Fuels, 29, 3366−3376.

Nawaf, A.T., Jarullah, A.T., Saba A.G., Mujtaba, I.M., (2015a). Development of Kinetic and Process Models for the Oxidative Desulfurization of Light Fuel, Using Experiments and the Parameter Estimation Technique. Ind. Eng. Chem. Res., 54, 12503−12515.

Patience, G. S., Chaouki, J., Berruti, F., Wong, R. (1992). Scaling considerations for circulating fluidized bed risers. *Powder technology*, *72*(1), 31-37.

Papayannakos, N., Georgiou, G. (1988). Kinetics of hydrogen consumption during catalytic hydrodesulphurization of a residue in a trickle-bed reactor. *Journal of chemical engineering of Japan*, *21*(3), 244-249.

Penteado, J. C., Rossi, L. F., Negrão, C. O. (2003). Numerical Modelling Of A Fcc Regenerator. In *In17th International Congress of Mechanical Engineering (COBEM 2003), Sao Paulo, Brazil*.

Pradhan, K. (2012). Simulation of fluid catalytic cracker. National Institute Of Technology, Rourkela.

Praveen, C. H., Shishir, S. (2009). Effect of pressure on height of regenerator dense bed in an FCCU. *J. Pet. Coal*, *51*(2), 124-135.

Rabinovich, E., Kalman, H. (2011). Flow regime diagram for vertical pneumatic conveying and fluidized bed systems. *Powder Technology*, *207*(1), 119-133.

Rankovic, N., Bourhis, G., Loos, M., Dauphin, R. (2015). Knock management for dual fuel SI engines: RON evolution when mixing low RON base fuels with octane boosters. *Fuel*, *150*, 41-47.

Reza, S. (2000). Fluid Catalytic Cracking Handbook. *Gulf Publishing*.

Sadeghbeigi, R. (2000). Fluid Catalytic Cracking Handbook Design. *Operation and Troubleshouting of FCC facilities, 2nd Ed., Gulf.*

Shuyan, W. A. N. G., Huilin, L. U., Jinsen, G. A. O., Chunming, X., & Dan, S. U. N. (2008). Numerical predication of cracking reaction of particle clusters in fluid catalytic cracking riser reactors. *Chinese Journal of Chemical Engineering*, *16*(5), 670-678.

Souza, J. A., Vargas, J. V. C., Meien, O. F. V., Martignoni, W. P. (2003). Numerical simulation of FCC risers. *Revista da Engenharia Térmica.*, 2(3), 17-21.

Speight, J. G. (2010). The refinery of the future, William Andrew.

Stratiev, D. Dinkov, R. (2007). Evaluation of FCC unit process variables impact on yield distribution and product quality part I. Evaluation of FCC unit variables impact on yield distribution. *Petroleum & Coal*, 49(1)**,** 71-77.

Svoboda, K., Kalisz, S., Miccio, F., Wieczorek, K., Pohořelý, M. (2009). Simplified modeling of circulating flow of solids between a fluidized bed and a vertical pneumatic transport tube reactor connected by orifices. *Powder Technology*, *192*(1), 65-73.

Twaiq, F. A. A., Bhatia, S., Zabidi, N. A. M. (2001). Catalytic cracking of palm oil over zeolite catalysts: statistical approach. *IIUM Engineering Journal*, *2*(1).

Wang, B., Zhu, J., Ma, H. (2009). Desulfurization from thiophene by SO 4 2−/ZrO 2 catalytic oxidation at room temperature and atmospheric pressure. *Journal of hazardous materials*, *164*(1), 256-264.

Watanabe, K., Nagai, K., Aratani, N., Saka, Y., Chiyoda, N., Mizutani, H. (2010). Techniques for Octane Number Enhancement in FCC Gasoline. In *Proceedings of 20th Annual Saudi-Japan Symposium on Catalysts in Petroleum Refining and Petrochemicals, Dhahran, Saudi Arabia, December*.

Weekman Jr., V. W. (1968). Model of catalytic cracking conversion in fixed, moving, and fluid-bed reactors. *Industrial & Engineering Chemistry Process Design and Development*, *7*(1), 90-95.

Werther, J., Hirschberg, B. (1997). Solids Motion And Mixing. Circulating Fluidized Beds. Chapman & Hall, Springer, Netherlands.

Xiong, K., Lu, C., Wang, Z., Gao, X. (2015). Kinetic study of catalytic cracking of heavy oil over an in-situ crystallized FCC catalyst. *Fuel*, *142*, 65-72.

List of Tables

List of Figures

Table 1: Specifications of the experimental apparatus **(Xiong et al., 2015)**

Specifications	**Values**
Length of reactor	65 cm
diameter of reactor	1.5 cm
Volume of catalyst in bed	65 cm^3

Table 2: Values of constant parameters and coefficients used in this model.

Parameter	**Symbol**	**Unit**	**Value**
Gas constant	R	$J/mole.K$	8.314
Critical volume of liquid vacuum gas oil	$v_c{}^L$	$cm^3/gmole$	1190
Molecular weight Vacuum gas oil, VGO	MW_{VGO}	$gm/gmole$	400
Molecular weight Light cycle oil, LCO	MW_{LCO}	$gm/gmole$	200
Molecular weight Gasoline, GLN	MW_{GLN}	$gm/gmole$	100
Molecular weight Liquefied petroleum gases, LPG	MW_{LPG}	$gm/gmole$	50
Molecular weight Dry gas, DG	MW_{DG}	$gm/gmole$	25
Molecular weight Coke, Ck	MW_{CK}	$gm/gmole$	400
Volume of catalyst	V_{cat}	cm^3	65
Catalyst bulk density	ρ_{cat}	gm/cm^3	0.9
pressure of reactor	P_r	atm	2.28
Diameter of catalyst particle	d_p	cm	0.0075
Total geometric volume of catalyst particle	V_P	cm^3	1.78×10^{-6}
Total geometric surface area of catalyst particle	S_P	cm^2	7.06×10^{-4}
Specific surface area of particle	S_g	cm^2/gm	388.8×10^{2}
Total pore volume	V_g	cm^3/gm	0.37
Regenerator pressure	P_{reg}	atm	2.588
weight fraction of H_2 in coke	C_H	$(-)$	0.165
relative (catalytic) CO combustion	X_{pt}	$(-)$	0.10
Deactivation order	d	$(-)$	1.6

Table 3: Values of constant cracking factors used in this model

Parameters	**Value**
$b_{VGO\rightarrow LCO}$	-1.5
$b_{VGO\rightarrow GLN}$	1.62
$b_{VGO\rightarrow LPG}$	1.7
$b_{VGO\rightarrow DG}$	0.14
$c_{i\rightarrow LCO}$	-0.43
$c_{i\rightarrow GLN}$	-0.42
$c_{i\rightarrow LPG}$	-0.52
$c_{i\rightarrow DG}$	-0.22
$c_{i\rightarrow CK}$	-0.43
$\mathrm{Log}(a_{\Delta H})$	2.0116
$\mathrm{Log}(b_{\Delta H})$	5.17720
$\mathrm{Log}(c_{\Delta H})$	7.7388

Table 4: Optimal kinetic parameters obtained for FCC model

Parameter	Symbol	Unit	Value
Order of vacuum gas oil concentration	n_1	(-)	0.925367
Order of light cycle oil concentration	n_2	(-)	1.000001
Order of Gasoline concentration	n_3	(-)	0.999785
Order of liquefied petroleum gases concentration	n_4	(-)	0.999413
Activation energy for reaction VGO→LCO	E_1	kJ/mole	20431.1
Activation energy for reaction VGO→GLN	E_2	kJ/mole	23082.6
Activation energy for reaction VGO→LPG	E_3	kJ/mole	23082.6
Activation energy for reaction VGO→DG	E_4	kJ/mole	22271.8
Activation energy for reaction VGO→CK	E_5	kJ/mole	9006.57
Activation energy for reaction LCO→GLN	E_6	kJ/mole	49215.6
Activation energy for reaction LCO→CK	E_7	kJ/mole	19854.4
Activation energy for reaction GLN→LPG	E_8	kJ/mole	70463.8
Activation energy for reaction GLN→DG	E_9	kJ/mole	88051.1
Activation energy for reaction LPG→DG	E_{10}	kJ/mole	65992.4
Pre-exponential factor for reaction VGO→LCO	A_1	$\left(\frac{cm^3}{gm}\right)^{0.074633} sec^{-1}$	8.15295×10^6
Pre-exponential factor for reaction VGO→GLN	A_2	$\left(\frac{cm^3}{gm}\right)^{0.074633} sec^{-1}$	391.828
Pre-exponential factor for reaction VGO→LPG	A_3	$\left(\frac{cm^3}{gm}\right)^{0.074633} sec^{-1}$	1276.72
Pre-exponential factor for reaction VGO→DG	A_4	$\left(\frac{cm^3}{gm}\right)^{0.074633} sec^{-1}$	1656.55
Pre-exponential factor for reaction VGO →Ck	A_5	$\left(\frac{cm^3}{gm}\right)^{0.074633} sec^{-1}$	1204.11
Pre-exponential factor for reaction LCO→GLN	A_6	sec^{-1}	598.233
Pre-exponential factor for reaction LCO→CK	A_7	sec^{-1}	20986.8
Pre-exponential factor for reaction GLN→LPG	A_8	$\left(\frac{cm^3}{gm}\right)^{0.000215} sec^{-1}$	3.0214×10^7
Pre-exponential factor for reaction VGO→DG	A_9	$\left(\frac{cm^3}{gm}\right)^{0.000215} sec^{-1}$	1.46191×10^7
Pre-exponential factor for reaction LPG→DG	A_{10}	$\left(\frac{cm^3}{gm}\right)^{0.000215} sec^{-1}$	28090.8
Sum of Square Errors	*SSE*	(-)	4.42621×10^{-7}

Table 5: Optimal operating conditions obtained for industrial FCC process

Operating conditions	Symbol	Unit	Values
Reaction Temperature	T_R	K	820.012
Weight Hourly Space Velocity	WHSV	hr^{-1}	2.002
Catalyst to Oil Ratio	CTO	(-)	10.00
Conversion	CV	(-)	87.6075
Octane number	Octane number	(-)	97.5722

Table 6: Comparison between the results obtained in this study and pervious work for vacuum gas oil conversion

Author(s) (year)	Conversion%
Ancheyta and Sotelo (2000)	78
Han et al. (2000)	80
Twaiq et al. (2001)	85
Han &Chung (2001a)	70
Han &Chung (2001b)	75
Fernandes et al. (2005)	75
This study (2016)	**87.61**

Table (7): Comparison between the results obtained in this study and pervious work for gasoline octane number

Author(s) (year)	Octane number
Li et al. (2003)	85
Stratiev & Dinkov (2008)	89
Svoboda et al. (2009)	92
Watanabe et al. (2010)	90
Rankovic et al. (2015)	91
This study (2016)	**97.57**

Table (8): Optimal operating conditions obtained for regenerated model

Variables	Symbol	Unit	Values
Coke in regenerated catalyst	C_{rge}	Wt%	0.000362
flow rate of air feed to the regenerator	F_{air}	Kmol s^{-1}	0.55
Regenerator temperature	T_{rge}	K	968.58

Table (9): Comparison between the results obtained in this study and pervious work for coke in regenerated catalyst

Author(s) (year)	Coke in regenerated catalyst (wt%)
Han and Chung, (2001b)	0.002
Souza et al. (2003)	0.012
Penteado et al. (2003)	0.016
Fernandes et al. (2005)	0.005
Fernandes et al. (2005a)	0.003
Shuyan et al.(2008)	0.100
Chuachuensuk et al.(2013)	0.015
This study (2016)	**0.000362**

Table 10: Comparison of the new results with those from other simpler models

Parameter	**Other models**	**This study**
Order of reactions	Usually are kept constant (assumed first or second order)	Have been estimated based on experiments with minimum errors
Effectiveness factor	Usually ignored	Has taken into accounts
Kinetic parameters	They are kept constant	Have estimated based on experiments
Catalyst deactivation	Generally has not taken into accounts	Has been taken into considerations
Physical properties	Usually are kept constant	Have been estimated as a function of operating conditions
Hydrodynamic parameters	Usually ignored	Has taken into accounts
Coke deposited	Mostly ignored	Have widely been studied
Estimation of kinetic parameters	Numerical methods	Advanced optimization technique

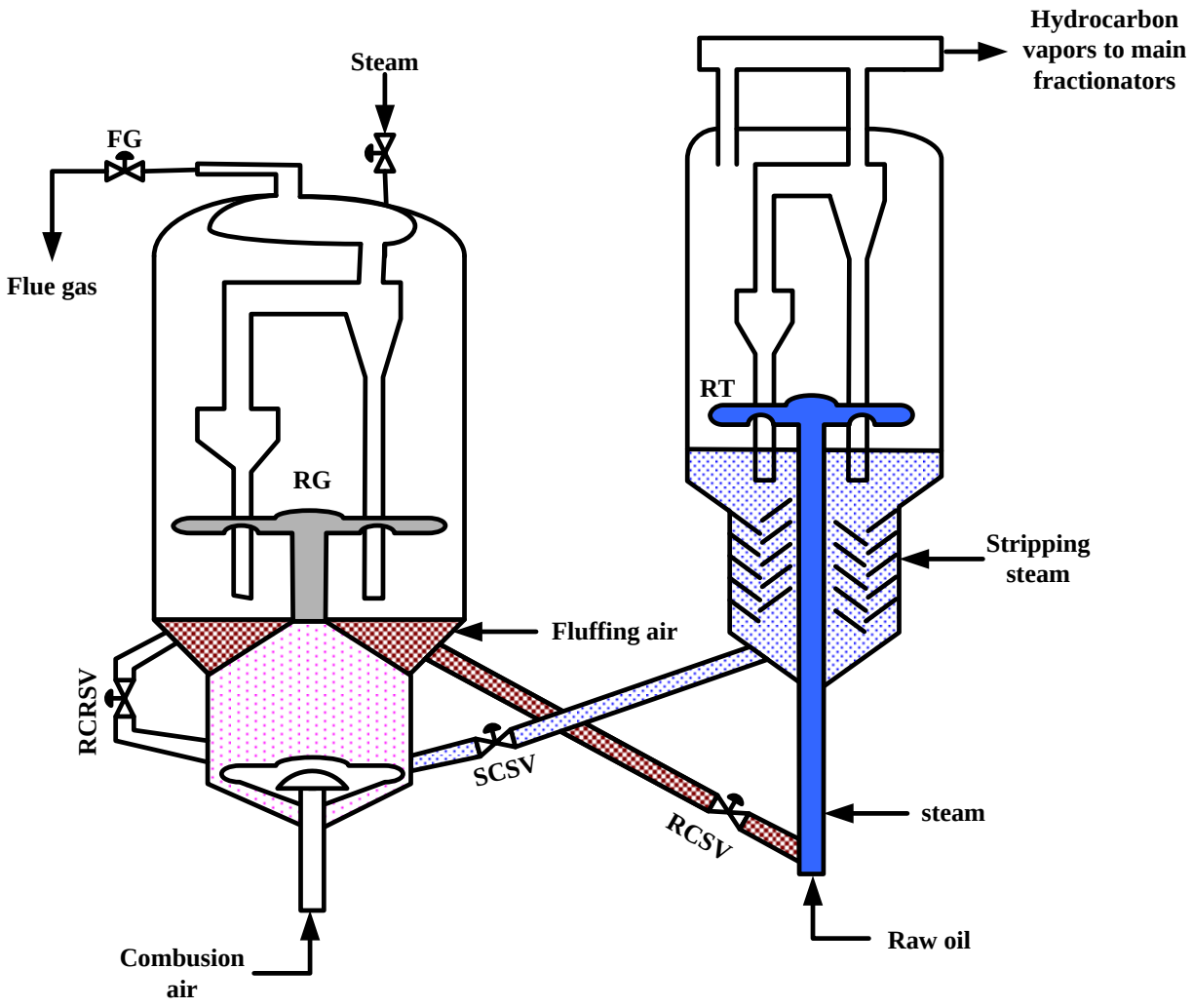

Figure 1: UOP fluid catalytic cracking unit **(Adapted from Fernandes et al., 2012)**

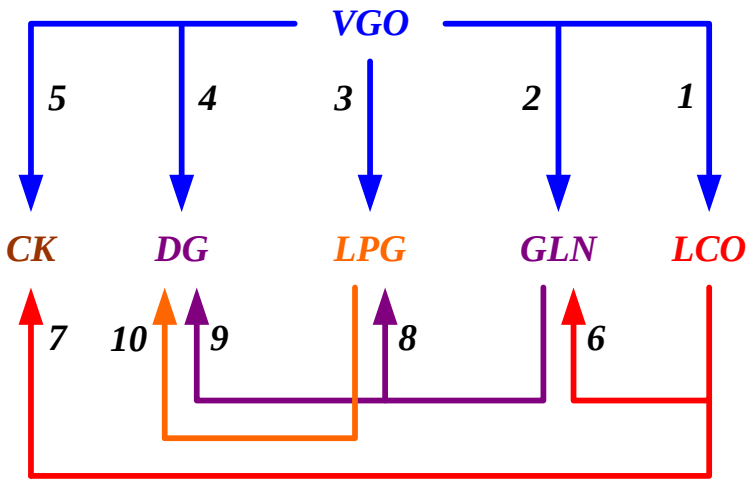

Figure 2: Kinetic scheme of propose the cracking reactions taking place in the riser

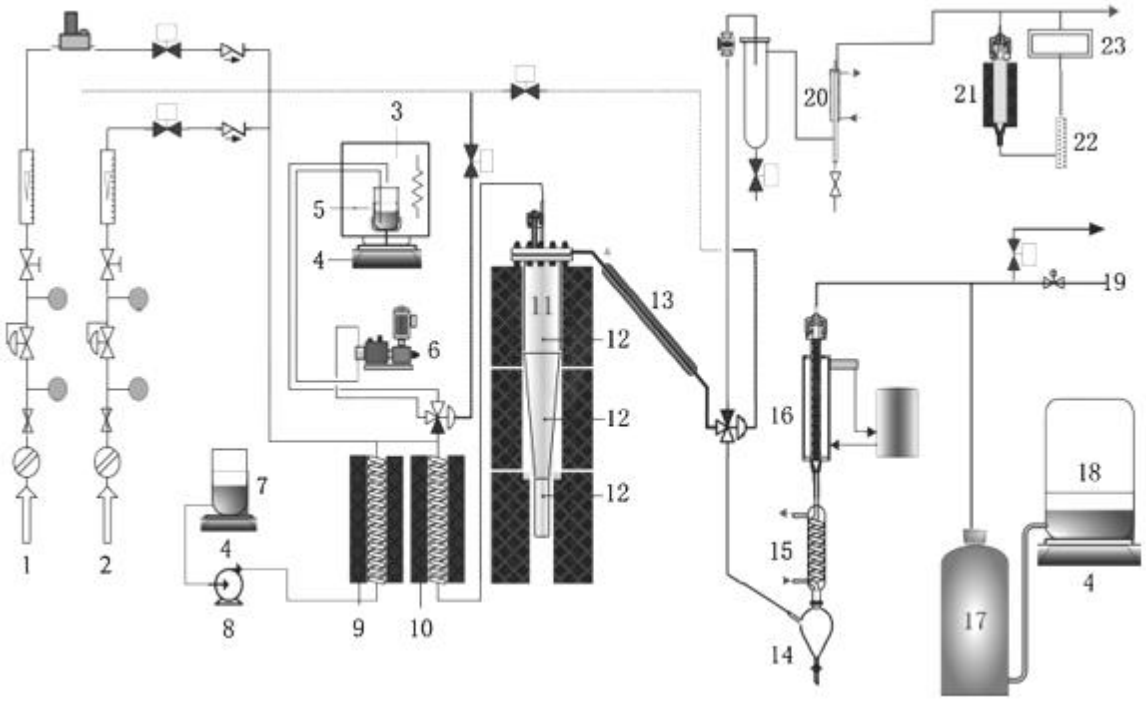

Figure 3: Schematic diagram for experimental setup: (1) oxygen; (2) air; (3) constant temperature box; (4) electronic balance; (5) feedstock; (6) oil pump; (7) water tank; (8) water pump; (9) steam generator; (10) preheater; (11) reactor; (12) thermocouple; (13) first condenser; (14) receiver for liquid products; (15) second condenser; (16) cold trap; (17) gas collection bottle; (18) water bottle; (19) gas sample connection; (20) drain sump; (21) CO converter; (22) drier; (23) CO 2 infrared detector.

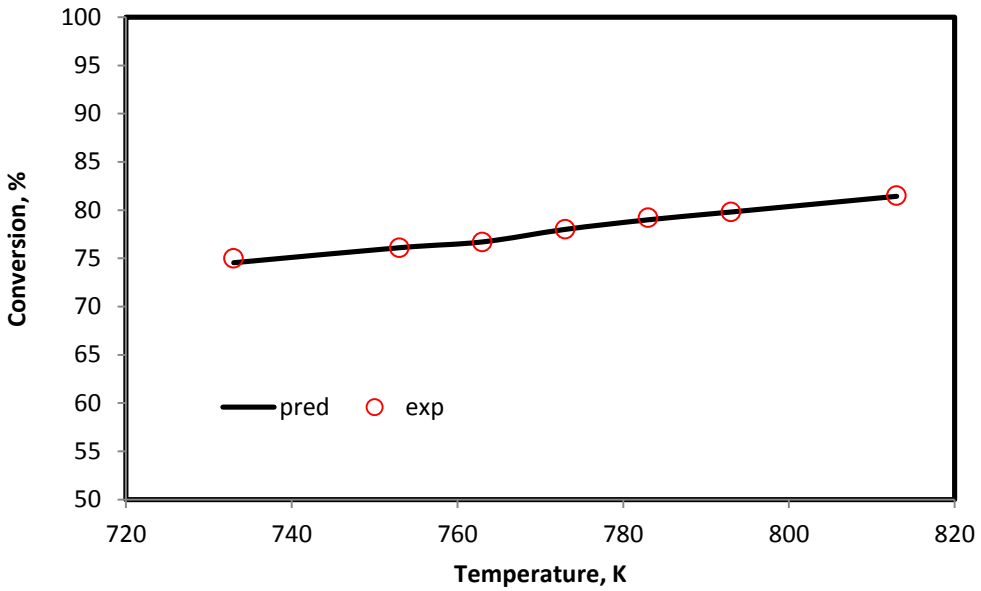

Figure 4: Effect of temperature on vacuum gas oil conversion at WHSV=15hr^{-1} and CTO=6

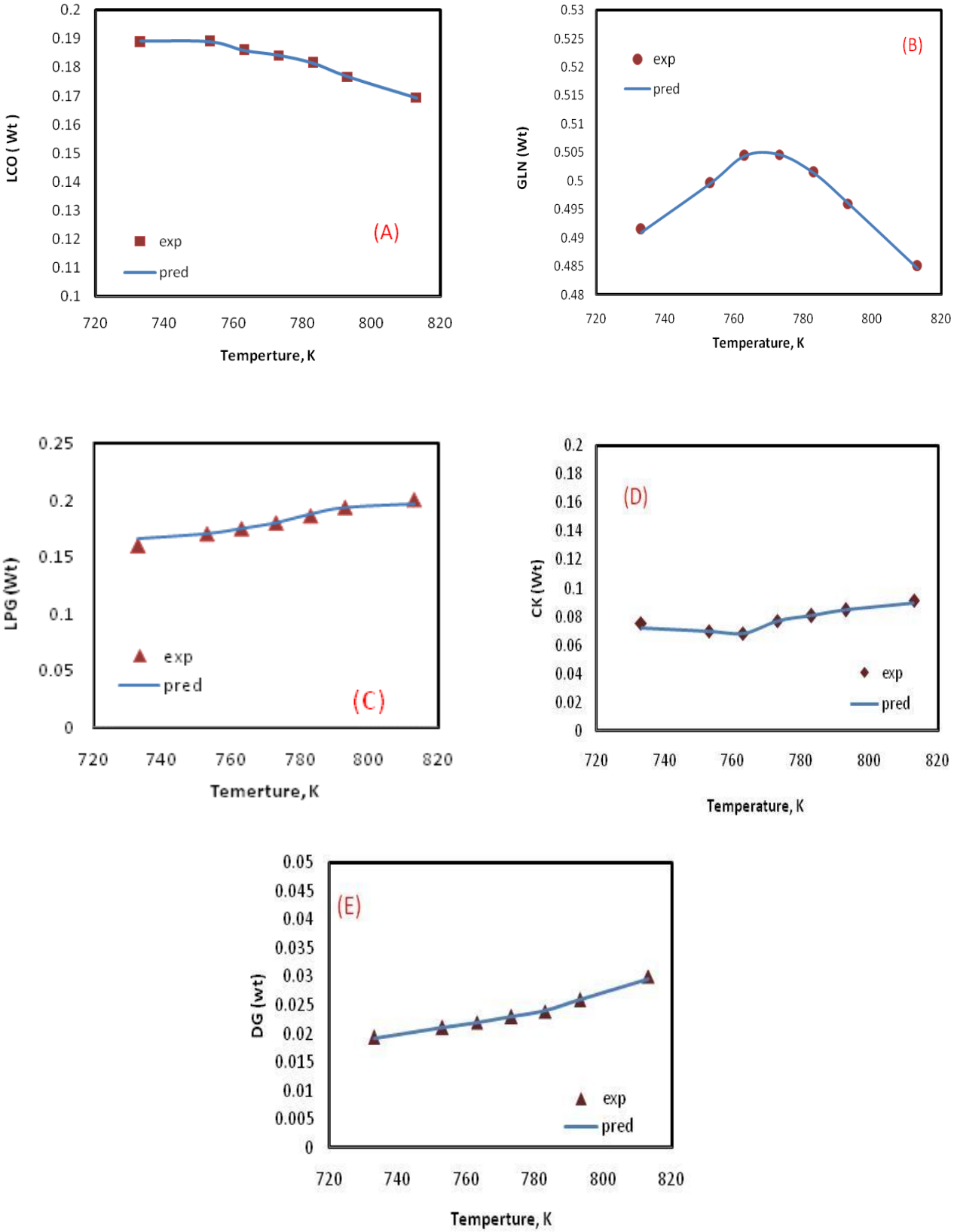

Figure 5: Effect of reaction temperature on product distribution (A (LCO), B (GLN), C (LPG), D(CK), E(DG)) at WHSV=15hr^{-1} and CTO=6

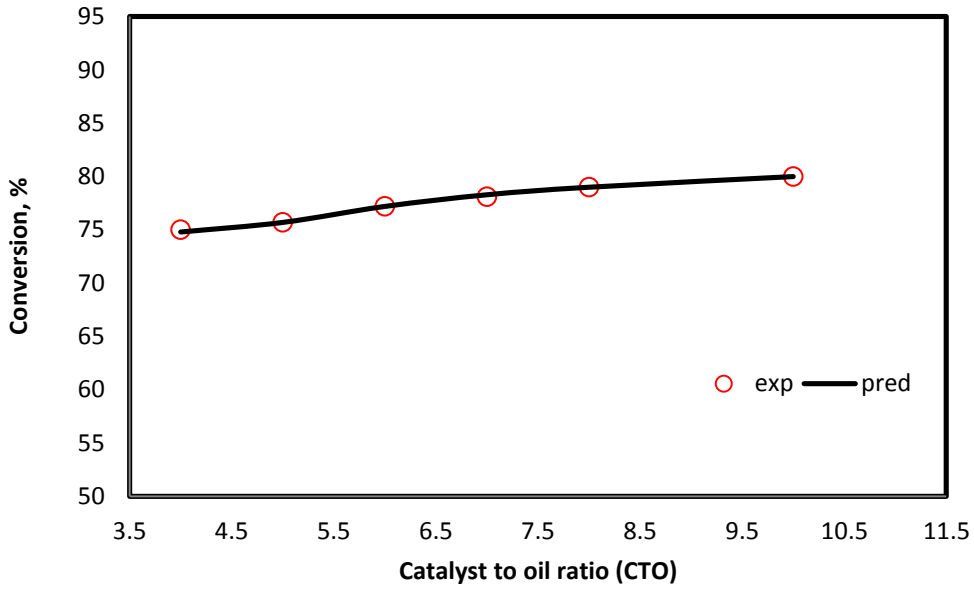

Figure 6: Effect of catalyst to oil ratio on vacuum gas oil conversion WHSV=15hr^{-1} and T=490ºC

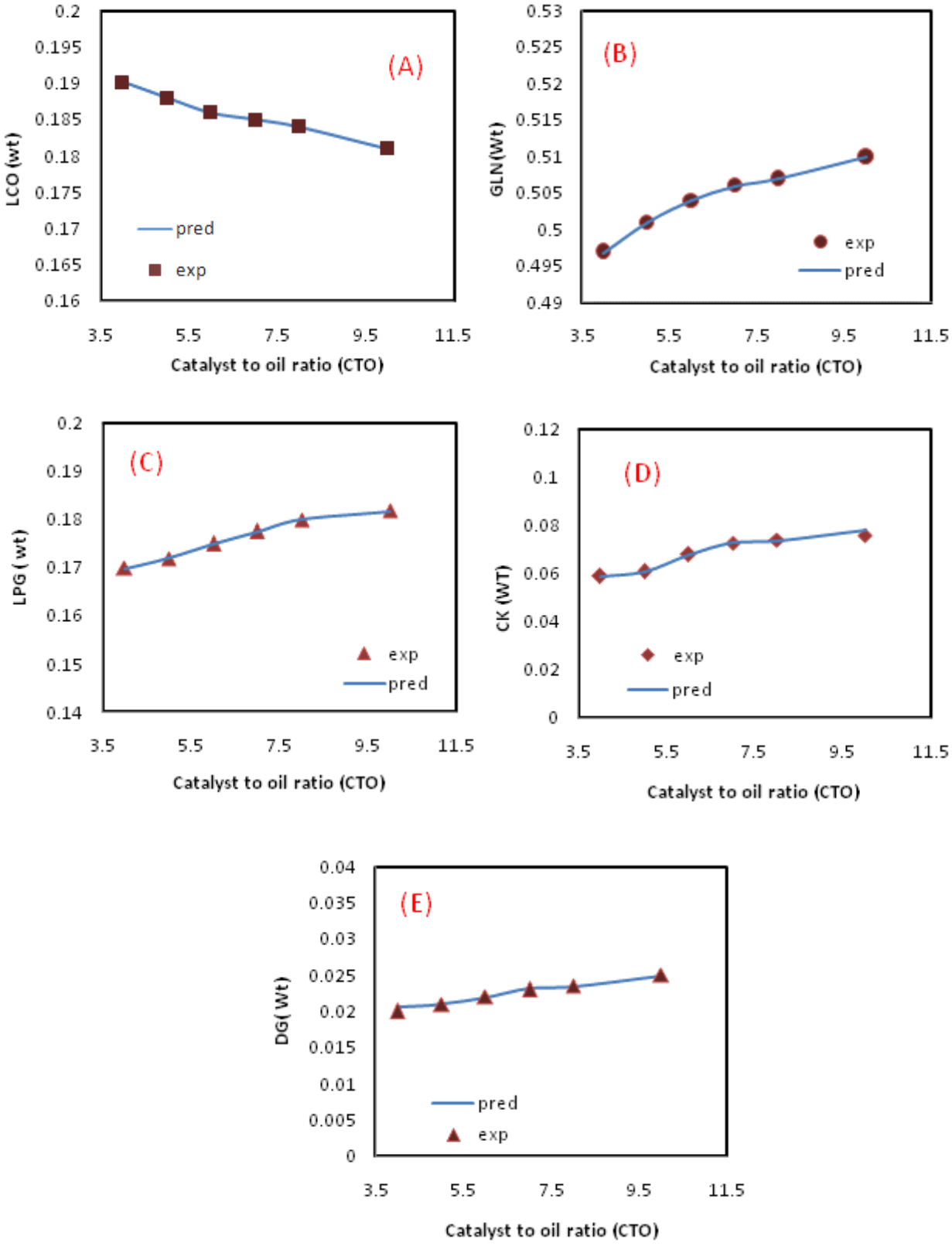

Figure 7: Effect of catalyst to oil ratio on product distribution (A (LCO), B (GLN), C(LPG), D(CK), E(DG)) at WHSV=15hr^{-1} and T=490 ºC

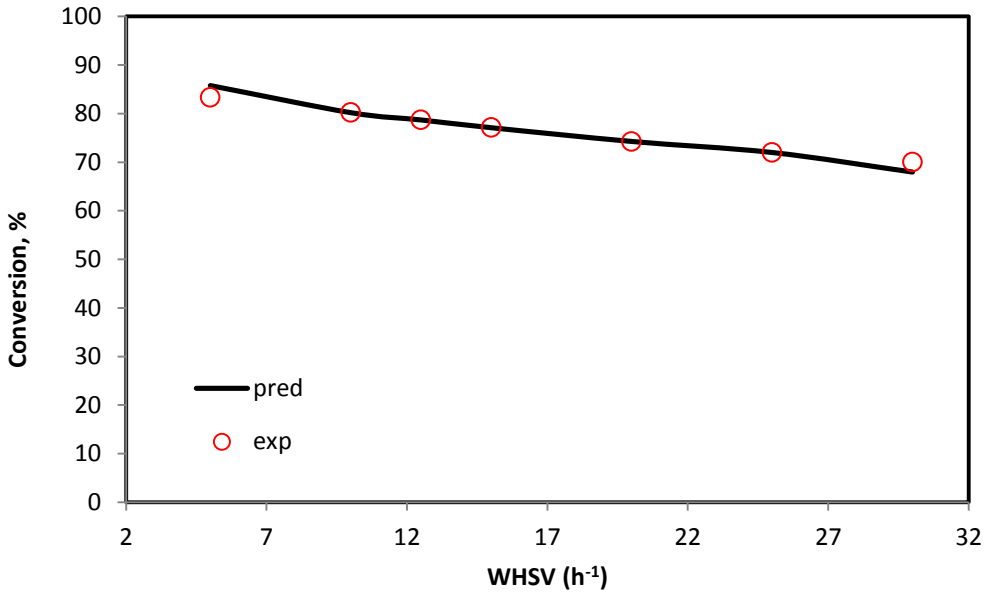

Figure 8: Effect of weight hourly space velocity on vacuum gas oil conversion at CTO=6 and T=490 ºC

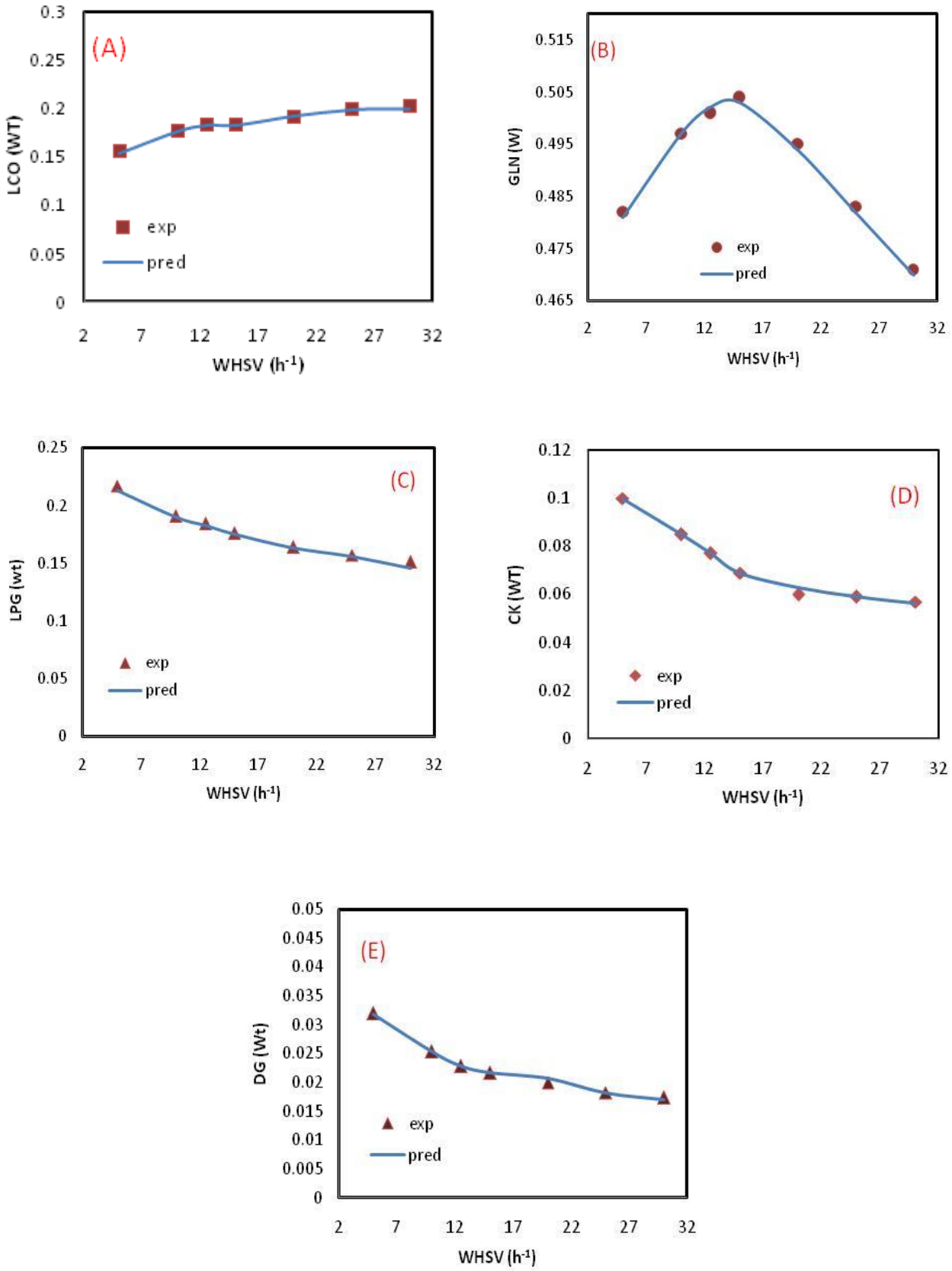

Figure 9: Effect of weight hourly space velocity WHSV on products distribution (A (LCO), B (GLN), C(LPG), D(CK), E(DG)) at CTO =6 and T=490 ºC

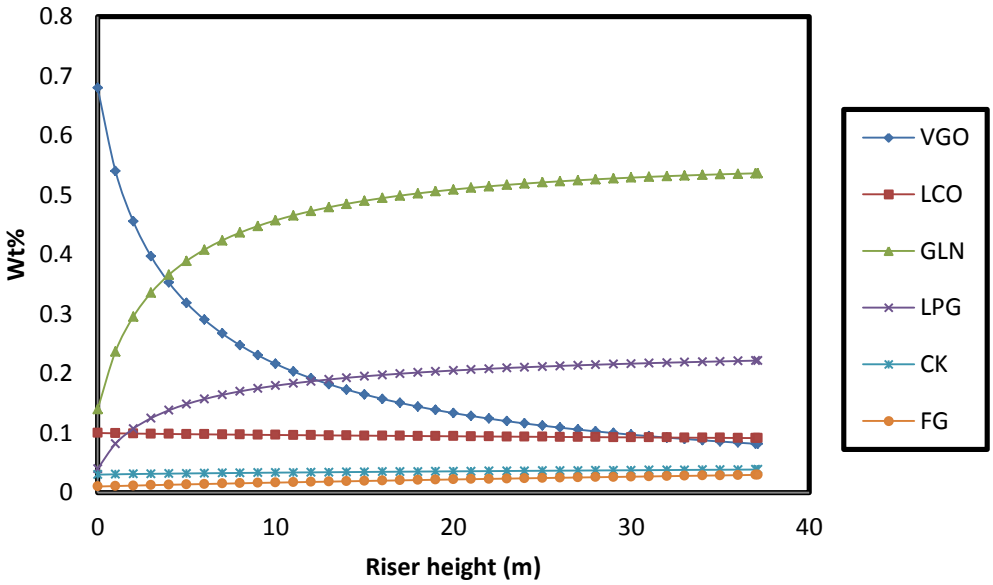

Figure 10: Six lumps concentration profile vs. riser height

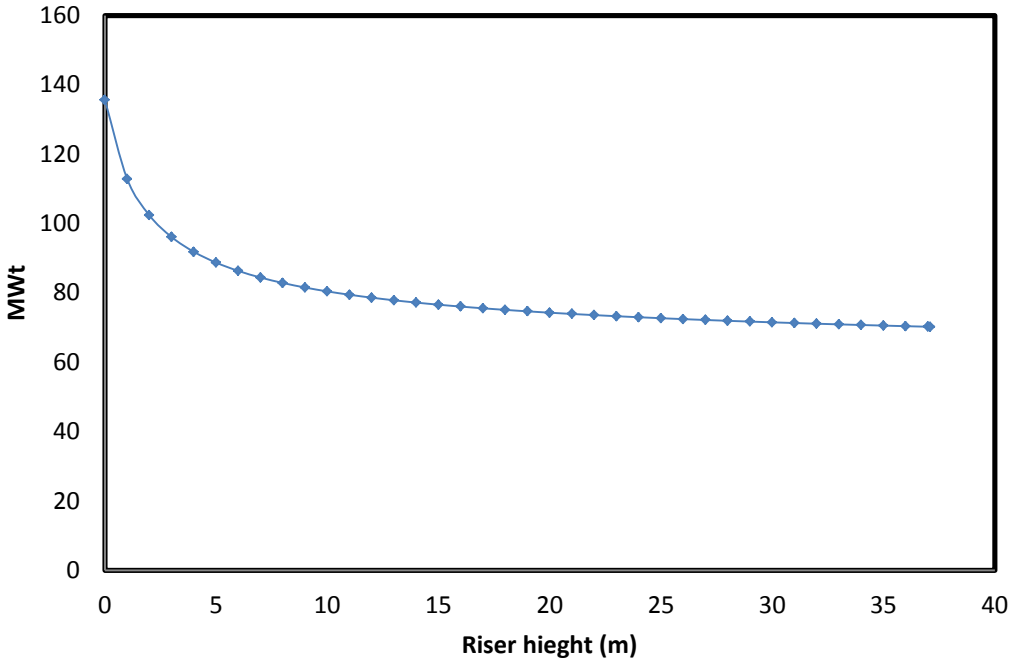

Figure 11: Gas phase molecular weight vs. riser length

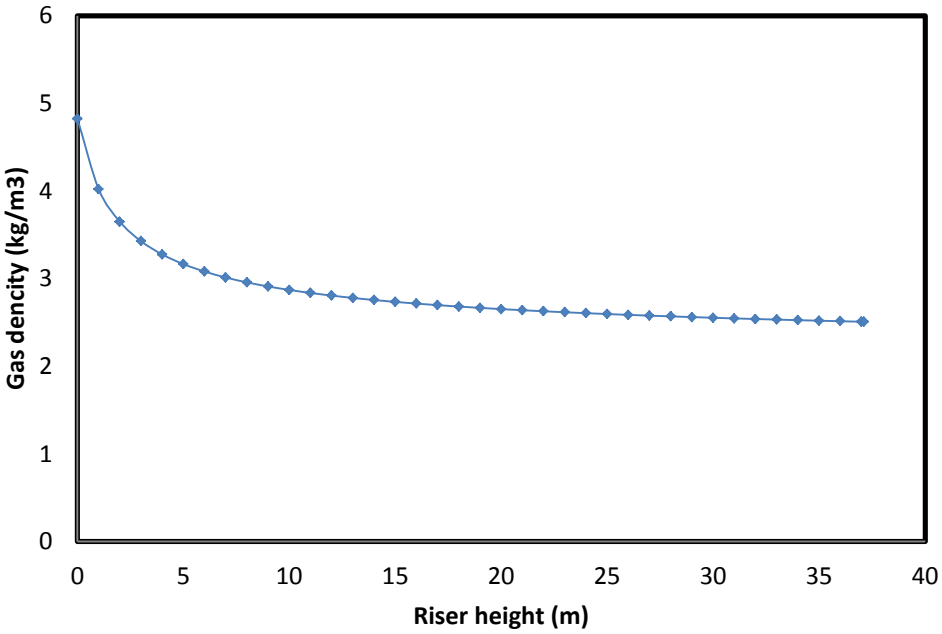

Figure 12: Gas phase density vs. height

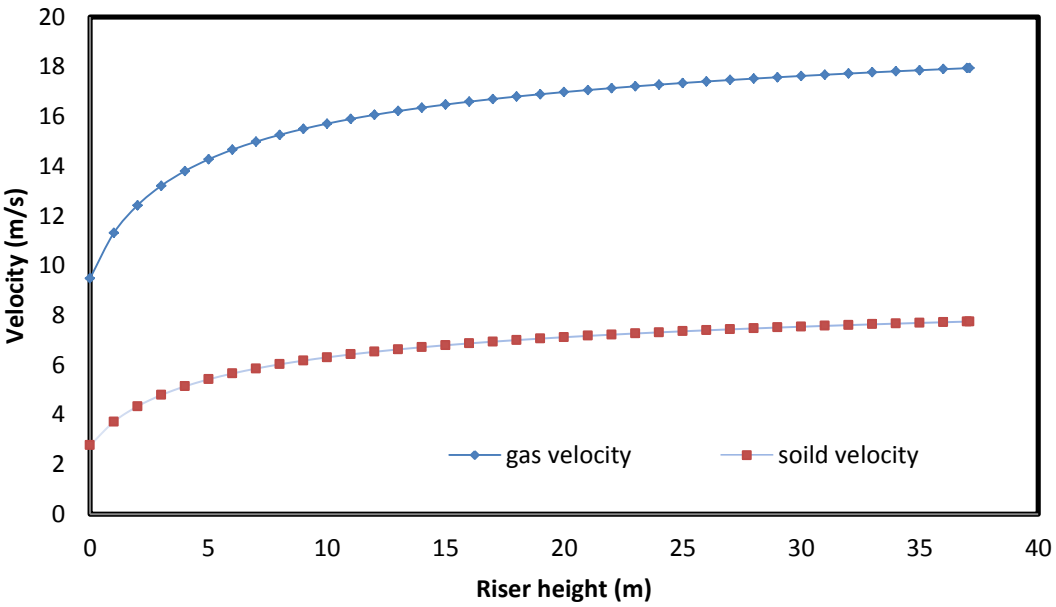

Figure 13: Gas phase and catalyst velocities vs. riser height

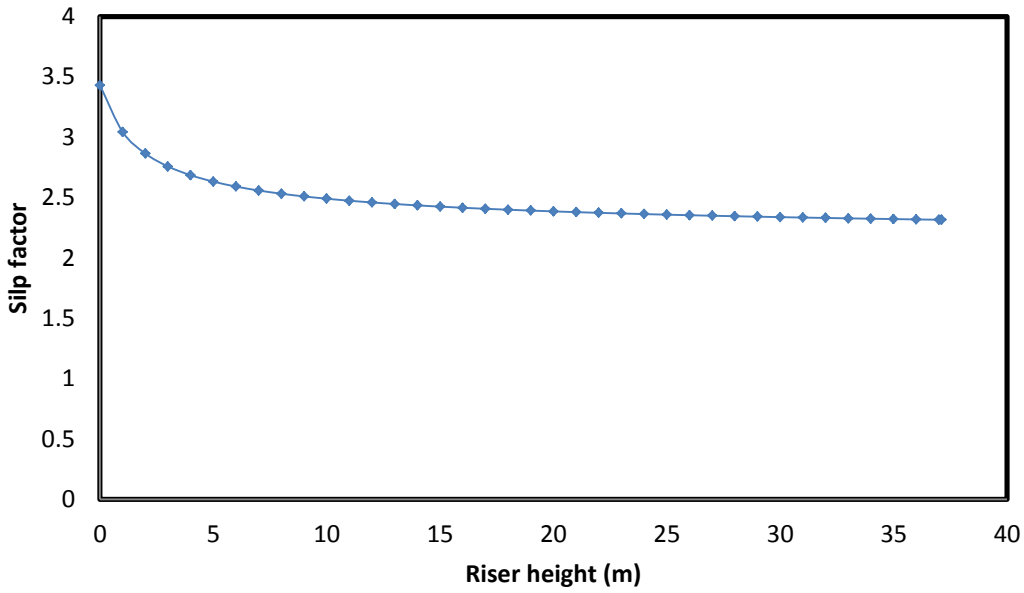

Figure 14: Slip factor vs. riser height